From Soft Clustering to Hard Clustering: A Collaborative Annealing Fuzzy c-Means Algorithm

Hongzong Li and Jun Wang, *Life Fellow, IEEE*

***Abstract*—The fuzzy c-means clustering algorithm is the most widely used soft clustering algorithm. In contrast to hard clustering, the cluster membership of data generated using the fuzzy c-means algorithm is ambiguous. Similar to hard clustering algorithms, the clustering results of the fuzzy c-means clustering algorithm are also suboptimal with varied performance depending on initial solutions. In this paper, a collaborative annealing fuzzy c-means algorithm is presented. To address the issue of ambiguity, the proposed algorithm leverages an annealing procedure to phase out the fuzzy cluster membership degree toward a crispy one by reducing the exponent gradually according to a cooling schedule. To address the issue of suboptimality, the proposed algorithm employs multiple fuzzy c-means modules to generate alternative clusters based on memberships repeatedly reinitialized using a metaheuristic rule. Experimental results on eight benchmark datasets are elaborated to demonstrate the superiority of the proposed algorithm to thirteen prevailing hard and soft algorithms in terms of internal and external cluster validity indices.**

***Index Terms*—Annealing procedure, collaborative clustering, fuzzy *c*-means (FCM) clustering, *k*-means (KM) clustering.**

I. Introduction

CLUSTERING is a popular unsupervised or semisupervised learning technique to explore the hidden structures of datasets. It is to group unlabeled data into multiple disjoint subsets with high intracluster similarity and low intercluster similarity. It arises in numerous applications, such as image segmentation [1], information retrieval [1], data mining [1], document clustering [2], video surveillance [2], feature selection [3], and pattern recognition [3].

Over the past decades, numerous clustering algorithms have been proposed, and they are mainly divided into two classes, including hard and soft clustering. Hard clustering is based on the assumption of mutually exclusive clusters, whereas soft clustering relaxes the assumption allowing overlapped clusters. In addition, hard clustering provides a simpler and more straightforward interpretation of the results, whereas soft clustering usually requires further interpretation and analysis to determine appropriate cutoff values for membership assignments.

Hard clustering assigns each datum to one and only one cluster. Hard clustering methods may be classified as full-space clustering algorithms, subspace clustering algorithms, feature-weighted clustering algorithms, and multiview clustering algorithms, depending on the feature spaces of their operations. Subspace clustering methods include the deep subspace clustering algorithm [4] and the robust possibilistic k-subspace clustering algorithm [5]. Feature-weighted clustering methods include the entropy weighting k-means (KM) clustering algorithm [6], the entropy-weighted power k-means (EWPKM) clustering algorithm [7], and the LASSO-weighted KM clustering algorithm [8]. Multiview clustering methods include the weighted multiview possibilistic c-means clustering algorithm with L2 regularization [9], and the multiview adjacency-constrained hierarchical clustering (HC) algorithm [10]. The hard clustering methods may be classified into hierarchical-based, center-based, distribution-based, and density-based clustering algorithms, according to the structure of the algorithms. HC-based methods cluster data based on the rule that closer data points exhibit more similarity to each other than the data points lying farther away, including divisive hierarchical algorithms [11] and agglomerative hierarchical algorithms [12]. The center-based clustering methods cluster data based on the rule that similarity is derived by the closeness of data to clusters, including KM [13], k-medoids algorithms [14], [15], k-harmonic means [16], and spectral clustering (SC) algorithms [17], [18], [19]. Distribution-based clustering methods cluster data based on the probability of data belonging to a specific distribution, including the expectation-maximization for Gaussian mixture model algorithms [20]. Density-based clustering methods cluster data based on the density of data points in the feature space, including the mean-shift algorithm [21], and the temporal streaming fuzzy density-based spatial clustering algorithm [22]. In addition, several collaborative clustering methods were proposed [23], including deep multiview collaborative clustering [24]. In spite of the progress, the clustering methods cannot guarantee the global optimality of clustering results. To mitigate the difficulty of discontinuity in the underlying objective function of KM, the power k-means

Manuscript received 9 April 2023; revised 5 July 2023 and 16 August 2023; accepted 23 September 2023. Date of publication 27 September 2023; date of current version 1 March 2024. This work was supported in part by the Research Grants Council of the Hong Kong Special Administrative Region of China under Grant 11202318, Grant 11202019, and Grant 11203721, and also in part by the InnoHK initiative, the Government of the Hong Kong Special Administrative Region, and the Laboratory for AI-Powered Financial Technologies. Recommended by Associate Editor W. Ding. *(Corresponding author: Jun Wang.)*

Hongzong Li is with the Department of Computer Science, City University of Hong Kong, Kowloon Tong, Hong Kong (e-mail: hongzli2-c@my.cityu.edu.hk).

Jun Wang is with the Department of Computer Science and School of Data Science, City University of Hong Kong, Kowloon Tong, Hong Kong (e-mail: jwang.cs@cityu.edu.hk).

This article has supplementary downloadable material available at https://doi.org/10.1109/TQE.2022.3153947, provided by the authors.

Color versions of one or more figures in this article are available at https://doi.org/10.1109/TFUZZ.2023.3319663.

Digital Object Identifier 10.1109/TFUZZ.2023.3319663

(PKM) algorithm clusters data by minimizing the majorization function of an annealed power-mean function [25]. Though the clustering performance using PKM is significantly improved, the clustering result is still suboptimal and dependent on initialization. To achieve optimal clustering results, the collaborative annealing power k-means++ (CAPKM++) algorithm clusters data by employing multiple PKM modules reinitialized using a particle swarm optimization rule [26]. CAPKM++ is demonstrated to outperform PKM and many other baselines [26]. As an upgraded version of CAPKM++, CAPKM++2.0 [27] is shown to be able to improve clustering efficiency via reinitialization during annealing [27].

As a relaxation of hard clustering, soft clustering allows each datum to belong to multiple clusters with membership degrees. Soft clustering methods include possibilistic clustering algorithms [28] and fuzzy clustering algorithms [29]. Possibilistic clustering methods include the robust automatic merging possibilistic clustering algorithm [30], the sparse possibilistic c-means algorithm [31], and the robust possibilistic k-subspace clustering algorithm [5]. Fuzzy clustering methods include the fuzzy c-means (FCM) algorithm [32], the centroid autofused hierarchical FCM clustering algorithm [33], fuzzy density peaks clustering [34], the robust jointly sparse fuzzy clustering algorithm [35], the fuzzy low-rank structural clustering algorithm [36], and the robust FCM algorithm [37]. Soft clustering introduces ambiguity in clustering results due to assigning each data point a membership value to each cluster. In addition, similar to existing hard clustering methods, the results of the soft clustering methods are also suboptimal.

FCM is one of the popular soft clustering methods due to its efficiency and simplicity [29]. However, it suffers the same drawback as other fuzzy clustering algorithms. To remedy the shortcoming of performance sensitivity to initialization, many alternative methods have been proposed, such as the FCM variants with improved objective function and initialization, and additional constraints. FCM-like algorithms with improved objective function include adaptive FCM algorithm [38], generalized FCM clustering [39], enhanced FCM [40], fast generalized FCM [41], fuzzy weighted c-means [42], [43], generalized FCM algorithm with improved fuzzy partition [44], fuzzy local information c-means [45], Bayesian fuzzy clustering (BFC) [46], and kernel fuzzy c-means clustering (KFCM) [47]. FCM with improved initialization includes multistage random sampling [48], the genetic algorithm [49], the Gustafson–Kessel algorithm [50], initialization schemes by utilizing color space in image segmentation [51], [52], the Markov random field [53], and the two-phase fuzzy c-means (2PFCM) [54]. Constrained FCM algorithms with additional constraints include the FCM method with spatial constraints [55], [56].

To achieve optimal clustering performance and eliminate the ambiguity in cluster membership and the dependency of performance on initial solutions, we propose the collaborative annealing fuzzy c-means based on FCM (CAFCM). An annealing procedure is used in CAFCM to phase out the fuzziness of cluster membership. In addition, multiple modules are employed to engender alternative clusters and reinitialized repeatedly using a metaheuristic rule to maximize clustering quality and eliminate the influence of initialization on clustering performance. The innovative contributions of this work are summarized as follows.

1) We theoretically prove that the underlying objective function of FCM is equivalent to that of PKM without annealing.
2) We propose CAFCM with a cooling schedule and experimentally demonstrate that the polynomial cooling schedule is the most cost-effective one.
3) We empirically estimate the computational complexity of CAFCM based on many datasets.
4) We experimentally demonstrate that CAFCM outperforms existing hard and soft clustering algorithms in terms of the mean values and standard deviations of many indices.

The rest of this paper is organized as follows. The related work on KM, FCM, PKM, CAPKM++, and CAPKM++2.0 is provided in Section II. The details of the CAFCM algorithm are presented in Section III. Experimental results on eight datasets are reported in Section IV. The paper is concluded in Section V.

II. Related Work

A. KM Algorithm

The KM algorithm is one of the most popular unsupervised learning algorithms. It groups the data into a preset number of clusters by minimizing the following objective function [13]:

$$f(\Theta) = \sum_{i=1}^{n} \min_{1\le j\le k} ||x_i - \theta_j||_2^2, \tag{1}$$

where $X = \{x_1, \ldots, x_n\} \in \Re^{n\times p}$ is an unlabeled dataset, n is the number of data points, k is the number of clusters, p is the number of features, $\Theta = [\theta_1, \ldots, \theta_k]$, and $\theta_j \in \Re^p$ is the j-th center.

B. FCM Algorithm

As an extension of KM, FCM was developed by Dunn [57], and improved by Bezdek [32]. Differing from KM that assigns each data point to exactly one cluster, FCM allows data points to belong to multiple clusters with different degrees of membership. It is based on the minimization of the following biconvex objective function [32]:

$$f_m(\mu, \Theta) = \sum_{i=1}^{n}\sum_{j=1}^{k} \mu_{ij}^m ||x_i - \theta_j||^2, \tag{2}$$

where $\mu_{ij} \in [0, 1]$ is the degree of membership of the i-th datum in the j-th cluster, $m > 1$ is an exponent for controlling the degree of fuzzy overlap, and θ_j is the center of the j-th cluster. The fuzzy objective function is subject to a constraint $\sum_{j=1}^{k} \mu_{ij} = 1\,(i = 1, \ldots, n)$; i.e., for each datum, the sum of the membership degrees over all clusters is one. For $j = 1, \ldots, k$, the centers are updated as follows [32]:

$$\theta_j = \frac{\sum_{i=1}^{n} \mu_{ij}^m x_i}{\sum_{i=1}^{n} \mu_{ij}^m}. \tag{3}$$

For $i = 1, \ldots, n$ and $j = 1, \ldots, k$, the degrees are updated alternatingly as follows [32]:

$$\mu_{ij} = \frac{1}{\sum_{l=1}^{k} \left(\frac{||x_i - \theta_j||}{||x_i - \theta_l||}\right)^{\frac{2}{m-1}}}. \tag{4}$$

Similar to KM, FCM iterates over (3) and (4) until no degree changes. Due to the biconvexity of the fuzzy objective function in (2), the alternating method cannot guarantee to converge to the global optimal cluster.

Note that $\lim_{m \to 1} \mu_{ij} \in \{0, 1\}$; i.e., FCM degenerates to KM [29].

C. PKM Algorithm

PKM [25] is proposed to improve KM algorithms by minimizing the following annealed power function:

$$f_s(\Theta) := \sum_{i=1}^{n} \left(\frac{1}{k} \sum_{j=1}^{k} ||x_i - \theta_j||_2^{2\,s} \right)^{\frac{1}{s}}, \tag{5}$$

where $s < 0$ denotes a power parameter.

Rather than minimizing the concave power-mean functions in (5), PKM minimizes the following convex majorization function [25]:

$$\hat{f}_s(\Theta) = \sum_{i=1}^{n} \sum_{j=1}^{k} w_{ij}(t) ||x_i - \theta_j(t+1)||_2^2. \tag{6}$$

The weights are updated as follows [25]:

$$w_{ij}(t) = \frac{||x_i - \theta_j(t)||^{2(s-1)}}{\left(\sum_{l=1}^{k} ||x_i - \theta_l(t)||^{2\,s}\right)^{1-\frac{1}{s}}}. \tag{7}$$

The clusters are updated as follows [25]:

$$\theta_j(t+1) = \frac{1}{\sum_{i=1}^{n} w_{ij}(t)} \sum_{i=1}^{n} w_{ij}(t) x_i.$$

The power parameter s is decreased at each step according to the following cooling schedule [25]:

$$s(t+1) = \eta s(t),$$

where $s(0) < 0$ and $\eta > 1$.

Let $s = -\frac{1}{m-1}$. The weight updating rule in (7) is rewritten as follows:

$$\begin{aligned} w_{ij} &= \frac{||x_i - \theta_j||^{2(s-1)}}{\left(\sum_{l=1}^{k} ||x_i - \theta_l||^{2\,s}\right)^{1-\frac{1}{s}}} \\ &= \frac{||x_i - \theta_j||^{-2\,m/(m-1)}}{\left(\sum_{l=1}^{k} ||x_i - \theta_l||^{-2/(m-1)}\right)^{m}}. \end{aligned} \tag{8}$$

Via substituting the weight updating rule in (8), the objective function in (5) is rewritten as follows:

$$\begin{aligned} \hat{f}_s(\Theta) &= \sum_{i=1}^{n} \sum_{j=1}^{k} w_{ij} ||x_i - \theta_j||^2 \\ &= \sum_{i=1}^{n} \sum_{j=1}^{k} \frac{||x_i - \theta_j||^{-2\,m/(m-1)}}{\left(\sum_{l=1}^{k} ||x_i - \theta_l||^{-2/(m-1)}\right)^{m}} \\ &\quad ||x_i - \theta_j||^2. \end{aligned} \tag{9}$$

The degree updating rule of FCM in (4) is rewritten as follows:

$$\begin{aligned} \mu_{ij} &= \frac{1}{\sum_{l=1}^{k} \left(\frac{||x_i - \theta_j||}{||x_i - \theta_l||}\right)^{\frac{2}{m-1}}} \\ &= \frac{||x_i - \theta_j||^{-2/(m-1)}}{\sum_{l=1}^{k} ||x_i - \theta_l||^{2/(m-1)}}. \end{aligned} \tag{10}$$

Via substituting degree updating rule (10), the objective function of FCM in (2) is rewritten as follows:

$$\begin{aligned} f_m(\mu, \Theta) &= \sum_{i=1}^{n} \sum_{j=1}^{k} \mu_{ij}^m ||x_i - \theta_j||^2 \\ &= \sum_{i=1}^{n} \sum_{j=1}^{k} \frac{||x_i - \theta_j||^{-2\,m/(m-1)}}{\left(\sum_{l=1}^{k} ||x_i - \theta_l||^{-2/(m-1)}\right)^{m}} \\ &\quad ||x_i - \theta_j||^2. \end{aligned} \tag{11}$$

It indicates that the objective functions of FCM in (2) and PKM in (6) are equivalent.

D. CAPKM++ and CAPKM++2.0 Algorithms

PKM is demonstrated in [25] to perform better than Lloyd's algorithm [13] and k-harmonic means [16]. Nevertheless, its clustering results are not globally optimal since its performance heavily depends on the anchor points where its majorization functions are located. To address the aforementioned issue, CAPKM++ [26] employs multiple PKM modules to generate centers for alternative clusters, and use a particle swarm optimization rule for repositioning the initial centers.

CAPKM++2.0 [27] is an upgraded version of CAPKM++. CAPKM++2.0 reinitializes the weights in the majorization function during annealing rather than reinitializing cluster centers after annealing. In addition, CAPKM++2.0 minimizes the power-mean functions directly instead of their majorization function as in PKM and CAPKM++. It is demonstrated in [27] that CAPKM++2.0 is more efficient than CAPKM++ in terms of algorithmic complexities.

III. Algorithm Description

The proposed CAFCM algorithm consists of triple loops: an FCM clustering loop, a reinitialization loop, and an annealing loop. In the FCM clustering loop, multiple FCM modules iterate until convergence. In the reinitialization loop, the FCM modules are reinitialized. In the annealing loop, an exponent $m(t)$ decreases iteratively. The fuzzy objective function in (2) is minimized during such an annealing process, similar to PKM [25], CAPKM++ [26], and CAPKM++2.0 [27]. As shown in Fig. 1, the following three types of cooling schedules may be used for the annealing of exponent $m(t)$. An exponential cooling schedule

$$m_e(t) = (m_e(0) - 1) \exp(-t) + 1. \tag{12}$$

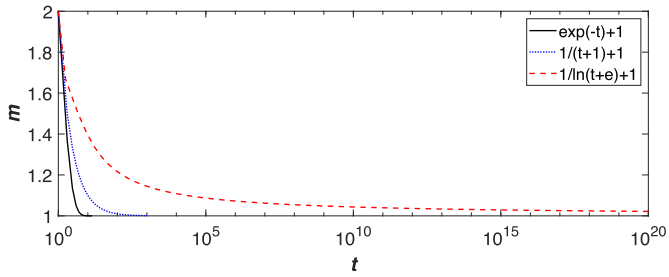

Fig. 1. Annealing curves of the three cooling schedules.

A polynomial cooling schedule

$$m_p(t) = \frac{m_p(0) - 1}{t + 1} + 1. \tag{13}$$

A logarithmic cooling schedule

$$m_l(t) = \frac{m_l(0) - 1}{\ln(t + e)} + 1. \tag{14}$$

Note that $\lim_{t\to\infty} m_e(t) = \lim_{t\to\infty} m_p(t) = \lim_{t\to\infty} m_l(t) = 1$. Each of the three cooling schedules has its pros and cons. As shown in Fig. 1, the exponential cooling schedule is the fastest, and it may cause prematurity in analogy to simulated annealing. The logarithmic cooling schedule is the slowest, and it takes a very long time to reduce to 1. The polynomial schedule is in-between.

In analogy to CAPKM++ [26] and CAPKM++2.0 [27], to overcome the biconvexity, $\mu(0)$ is repeatedly reinitialized according to the following particle swarm optimization rule in [58]:

$$v^{(i)}(t+1) = c_0 v^{(i)}(t) + c_1 r_1(\mu^{(i)*} - \mu^{(i)}(t)) \tag{15a}$$

$$+ c_2 r_2(\mu^{*} - \mu^{(i)}(t)), \tag{15b}$$

$$\mu^{(i)}(t+1) = \mu^{(i)}(t) + v^{(i)}(t+1), \tag{15c}$$

where $v^{(i)}(t)$ is an incremental vector of the i-th module, $\mu^{(i)*}$ is the current best degree vector of the i-th module, $\mu^{(i)}(t)$ is the current degree vector of the i-th module, μ^* is the current best degree vector of the multiple modules, $c_0 \in [0, 1]$ is a constant, c_1, c_2 are two positive constants, and r_1, r_2 are two random numbers in [0,1].

The high diversity of solutions is essential for improving clustering performance. A diversity measure of solutions is defined as follows:

$$\delta(\mu) = \frac{1}{Nnk} \sum_{j=1}^{N} \|\mu^{(j)} - \mu^{*}\|_2, \tag{16}$$

where N is the population size (i.e., the number of alternative cluster sets).

Mutation operation is a commonly used method to maintain a certain level of diversity and prevent premature convergence. If the diversity measure is below a threshold (i.e., $\delta(\mu) < \delta_{\min}$),

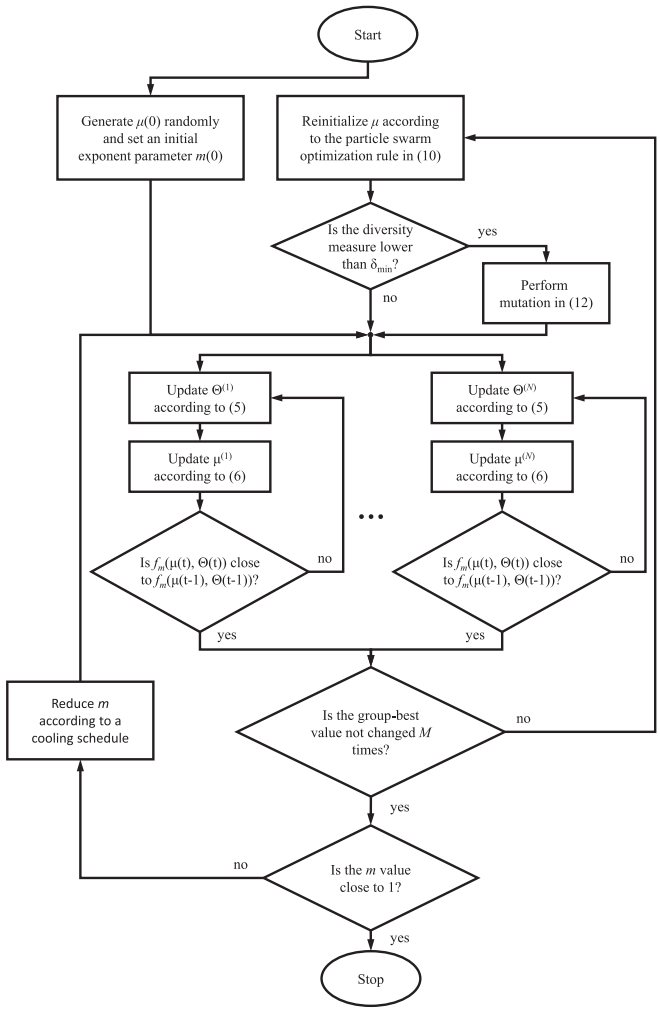

Fig. 2. Flowchart of CAFCM.

then a wavelet mutation operator is used to assure the diversity [59]

$$\mu^{(i)}(t+1) = \begin{cases} \mu^{(i)}(t) + \zeta(\overline{\mu}^{(i)} - \mu^{(i)}(t)) & \zeta > 0 \\ \mu^{(i)}(t) + \zeta(\mu^{(i)}(t) - \underline{\mu}^{(i)}) & \zeta < 0, \end{cases} \tag{17}$$

where $\overline{\mu}^{(i)} = 1$ and $\underline{\mu}^{(i)} = 0$ are the upper bound and lower bound of the membership degree of the i-th module, and ζ is defined by a wavelet function

$$\zeta = \frac{1}{\sqrt{a}} \exp -\frac{1}{2}\left(\frac{\psi}{a}\right)^2 \cos\left(\frac{5\psi}{a}\right),$$

where $a = \exp(10(\ell/\ell_{\max}))$ is the amplitude of the wavelet function, $\ell_{\max}$ is the maximum iterative number, and ψ is the frequency of the wavelet function to be randomly generated from the interval $[-2.5a, 2.5a]$.

Fig. 2 portrays a flowchart of the CAFCM algorithm, and Algorithm 1 details its procedure. In Steps 6–10, centers Θ and degrees μ are updated alternately until convergence, where ϵ in Step 10 is to determine whether $f_m(\mu^{(i)}(\hat{t}), \Theta^{(i)}(\hat{t}))$ and $f_m(\mu^{(i)}(\hat{t}-1), \Theta^{(i)}(\hat{t}-1))$ are close enough. In Steps 11–13, the individual best degrees $\tilde{\mu}^{(i)}$ are determined. In Steps 15–21,

Algorithm 1: CAFCM.

Input: M, N, $m(0)$, c_0, c_1 and c_2, $X \in \mathbb{R}^{n\times p}$. particle/group best degrees $\tilde{\mu}^{(p)}$/ μ^*, $f(\tilde{\mu}^{(p)}) = f(\mu^*) = \infty$, initial degrees $[\mu^{(1)}(0), ..., \mu^{(N)}(0)]$, initial incremental vector $[v^{(1)}(0), ..., v^{(N)}(0)]$,

Output: μ^*.

1 $t \leftarrow 0$;
2 **repeat**
3 **while** $l \leq M$ **do**
4 **for** $i = 1$ **to** N **do**
5 $\hat{t} \leftarrow 1$;
6 **repeat**
7 Update $\Theta^{(i)}(\hat{t})$ according to Eqn. (3);
8 Update $\mu^{(i)}(\hat{t})$ according to Eqn. (4);
9 $\hat{t} \leftarrow \hat{t} + 1$;
10 **until** $|f_m(\mu^{(i)}(\hat{t}), \Theta^{(i)}(\hat{t})) - f_m(\mu^{(i)}(\hat{t}-1), \Theta^{(i)}(\hat{t}-1))| < \epsilon$;
11 **if** $f(\mu^{(i)}) < f(\tilde{\mu}^{(i)})$ **then**
12 $\tilde{\mu}^{(i)} \leftarrow \mu^{(i)}$;
13 **end**
14 **end**
15 $i^* = \arg\min_i\{f(\mu^{(1)}), ..., f(\mu^{(i)}), ..., f(\mu^{(N)}\}$;
16 **if** $f(\mu^{(i^*)}) < f(\mu^*)$ **then**
17 $\mu^* \leftarrow \mu^{(i^*)}$;
18 $l \leftarrow 0$;
19 **else**
20 $l \leftarrow l + 1$;
21 **end**
22 **for** $i = 1$ **to** N **do**
23 Update $v^{(i)}$ according to Eqn. (15a);
24 Update $\mu^{(i)}$ according to Eqn. (15c);
25 **end**
26 Compute $\delta(\mu)$ according to Eqn. (16);
27 **if** $\delta(\mu) < \delta_{\min}$ **then**
28 Perform mutation according to Eqn. (17);
29 **end**
30 **end**
31 $t \leftarrow t + 1$;
32 Reduce $m(t)$ according to Eqn. (12), Eqn. (13), or Eqn. (14);
33 **until** $m(t) - 1 < \epsilon$;
34 **return** μ^*.

the group best degrees μ^* are determined and the termination counter is updated. In Steps 22–25, the degrees are reinitialized according to (15). In Step 26, the diversity of the N sets of degrees is measured according to (16). In Steps 27–29, the wavelet mutation operator in (17) is performed if the diversity measure is below the preset threshold $\delta_{\min}$. In Step 32, the exponent m is reduced according to one of the three cooling schedules. In Step 10, the termination condition whether m is close to 1 is determined. The code of CAFCM is available in Github.[1]

[1][Online]. Available: https://github.com/HongzongLI-CS/CAFCM-Github

TABLE I
INFORMATION ABOUT THE EIGHT BENCHMARK DATASETS AND THE CORRESPONDING HYPER-PARAMETER VALUES USED IN CAFCM

Datasets	n	p	k	N	M
NCI9[2][60]	60	9712	9	2	10
WarpPIE10P[3][60]	210	2420	10	2	5
WQ-White[4][61]	4898	11	11	2	15
PageBlocks[5][61]	5472	10	5	2	5
Texture[6][61]	5500	40	11	3	15
Optdigits[7][61]	5620	65	10	2	5
EGS[8][62]	10000	13	2	2	5
LR[9][63]	20000	16	26	3	15

[2] [Online]. Available: https://jundongl.github.io/scikit-feature/files/datasets/nci9.mat
[3] [Online]. Available: https://jundongl.github.io/scikit-feature/files/datasets/warpPIE10P.mat
[4] [Online]. Available: https://sci2s.ugr.es/keel/dataset.php?cod=209
[5] [Online]. Available: https://sci2s.ugr.es/keel/dataset.php?cod=104
[6] [Online]. Available: https://sci2s.ugr.es/keel/dataset.php?cod=72
[7] [Online]. Available: https://sci2s.ugr.es/keel/dataset.php?cod=199
[8] [Online]. Available: https://archive.ics.uci.edu/ml/datasets/Electrical+Grid+Stability+Simulated+Data+
[9] [Online]. Available: https://archive.ics.uci.edu/ml/datasets/Letter+Recognition

IV. EXPERIMENTAL RESULTS

In the experiments, the CAFCM parameters are set as follows. The value of the initial exponent $m(0)$ is set to 2, as in most of the existing references. The diversity threshold $\delta_{\min}$ is set to a sufficiently small value (i.e., 10^{-3}). In the FCM clustering loop of CAFCM, the parameter ϵ is also set to a sufficiently small value (i.e., 10^{-3}) as a stopping criterion of cluster membership updating. In the particle swarm optimization rule in (15), c_0, c_1, and c_2 are set to 1, as typically in many references, e.g., in [26] and [27].

A. Cooling Schedules

In this section, we compare the performances of CAFCM with the three cooling schedules. To make a fair comparison, the three cooling schedules are set to the same number of iterations. Since the logarithmic cooling schedule takes a long time for $m(t)$ to reduce to 1, instead of iterating over every t, sampling time $\tau(t)$ is used under the condition that the value of $m_l(\tau)$ is larger than that of the polynomial cooling schedule at every sampling time (i.e., $m_l(\tau(t)) > m_p(t)$) to keep its annealing process slower than the polynomial one. Since $\frac{m_p(0)}{t+2} > \frac{m_p(0)-1}{t+1}$ for $t > m_p(0) - 1$, letting $\frac{m_l(0)-1}{\ln(\tau(t)+e)} + 1 = \frac{m_p(0)}{t+2} + 1$ enables $m_l(\tau(t)) > m_p(t)$. The solution to the equation is $\tau(t) = \exp(\frac{(m_l(0)-1)(t+2)}{m_l(0)}) - e$, assuming that $m_l(0) = m_p(0)$.

The experimental results are based on eight commonly used datasets summarized in Table I. In addition, to show the superiority of CAFCM with the logarithmic cooling schedule on the dataset that is difficult to cluster, a dataset under uniform distribution (UDD) is generated, where $n = 5\,000$ and $p = 2$.

Fig. 3 shows 20-run Monte Carlo test results of CAFCM ($N = 2$ and $M = 5$) with the three cooling schedules on the six datasets in Table I and the UDD. As shown in Fig. 3, CAFCM with the polynomial cooling schedule or the logarithmic cooling

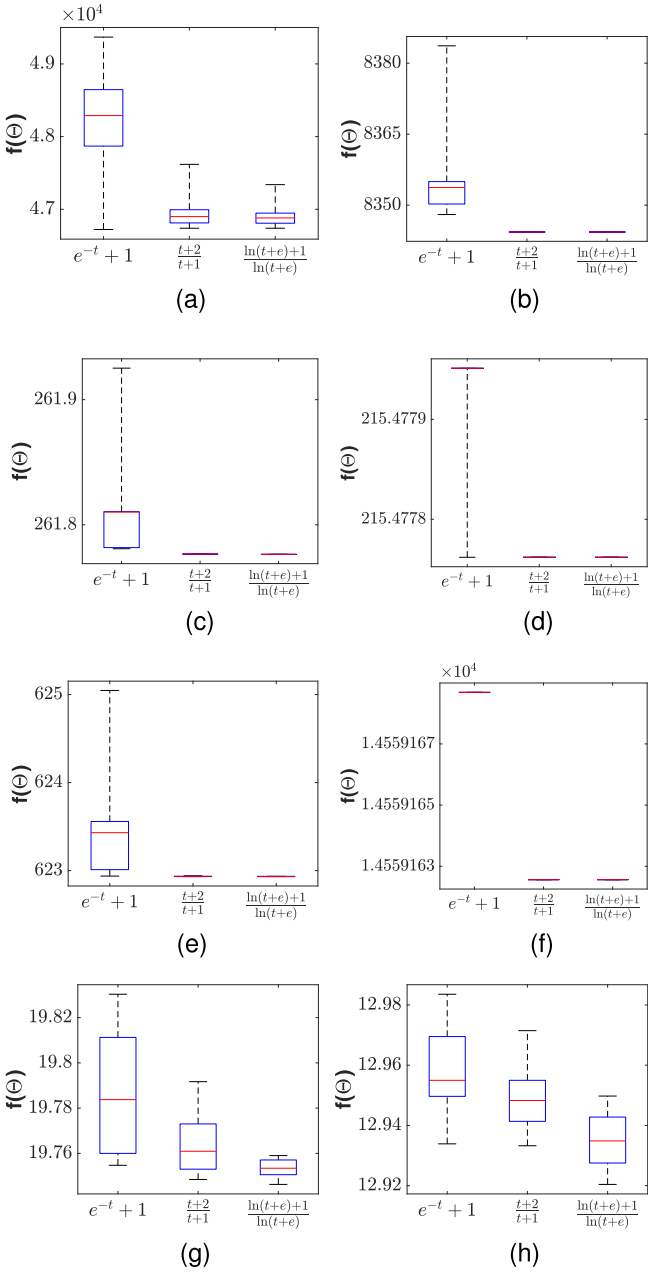

Fig. 3. Monte Carlo test results of CAFCM ($N = 2$ and $M = 5$) with the three cooling schedules on the six datasets and the UDD with two different k values. (a) NCI9. (b) WarpPIE10P. (c) WQ-White. (d) PageBlock. (e) Texture. (f) Optdigits. (g) UDD ($k = 40$). (h) UDD ($k = 60$).

schedule outperforms that with the exponential cooling schedule. It is also shown in Fig. 3 that CAFCM with the logarithmic cooling schedule outperforms that with the polynomial cooling schedule on NCI9, Texture, and UDD, especially on the UDD, and the superiority is more evident for a larger k value on the UDD.

Although the performance of CAFCM with the logarithmic cooling schedule is better than that with the polynomial cooling schedule, it takes too long time to reach 1, or it is difficult to set a reasonable sampling time to achieve high performance. In view of the fact that CAFCM with the polynomial cooling schedule performs well on the six datasets in Table I, the polynomial cooling schedule $m_p(t)$ is used in all the other experiments.

B. Hyperparameters Selection

Similar to CAPKM++ [26] and CAPKM++2.0 [27], the values of two hyperparameters N and M in Algorithm 1 are selected based on 50-run Monte Carlo tests on the six datasets. Fig. 4 depicts the boxplots of the Monte Carlo test results obtained using the CAFCM algorithm over 20 runs on the six datasets. As shown in Fig. 4, the results of the objective function values reaching zero standard deviation with $N = 2$ and $M = 10$ on NCI9, $N = 2$ and $M = 5$ on WQ-White, $N = 2$ and $M = 15$ on WarpPIE10P, $N = 2$ and $M = 5$ on PageBlocks, $N = 3$ and $M = 15$ on Texture, and $N = 2$ and $M = 5$ on Optdigits. Table I tabulates the values of the two hyperparameters (i.e., N and M) used in CAFCM on the eight datasets.

C. Convergent Behaviors

Fig. 5 depicts twelve snapshots of the convergent centers Θ and the convergent degrees μ values in the FCM clustering loop (Steps 6–10) of CAFCM on the six datasets. Fig. 6 depicts the monotonically decreasing values of $f_m(\mu, \Theta)$ in (2) corresponding to Θ and μ in Fig. 5. They show that the centers and the degrees reach their equilibria and the fuzzy objective function values reach their minima with a range of 40–400 iterations in the FCM clustering loop of CAFCM.

Fig. 7 depicts the monotonically decreasing values of $f(\Theta)$ in the annealing loop (Steps 2–33) of CAFCM on the six datasets. It shows that CAFCM converges within 120 iterations on NCI9, 80 iterations on WarpPIE10P, 1 000 iterations on WineQuality-White, 30 iterations on PageBlocks, 160 iterations on Texture, and 1 500 iterations on Optidigits.

D. Performance Comparison

The clustering performance of CAFCM is compared with the following six fuzzy clustering algorithms and seven crisp clustering algorithm: KM,[10] k-mean++ (KM++),[11] PKM [25], EWPKM,[12] (SC,[13] HC,[14] CAPKM++2.0 [27], BFC [46], fuzzy subspace clustering (FSC) [64], maximum entropy clustering (MEC) [65], FCM,[15] KFCM [47], and 2PFCM [54]. The clustering results of the fuzzy clustering algorithms (i.e., BFC, FSC, MEC, FCM, KFCM, and 2PFCM) are determined by the maximum fuzzy membership degrees. The code of PKM is provided by the authors of [25]. The agglomerative HC algorithm is used. The code of BFC is obtained from a link in [46]. As BFC involves the Cholesky factorization of the covariance matrices of data, and the covariance matrices of some data are not positive

[10] [Online]. Available: https://www.mathworks.com/help/stats/kmeans.html?s_tid=srchtitle_kmean_1

[11] [Online]. Available: https://github.com/xuyxu/Clustering

[12] [Online]. Available: https://github.com/DebolinaPaul/EWP

[13] [Online]. Available: https://www.mathworks.com/help/stats/spectralcluster.html

[14] [Online]. Available: https://www.mathworks.com/help/stats/hierarchical-clustering.html?s_tid=srchtitle_hierarchical%20clustering_1

[15] [Online]. Available: https://www.mathworks.com/help/fuzzy/fcm.html

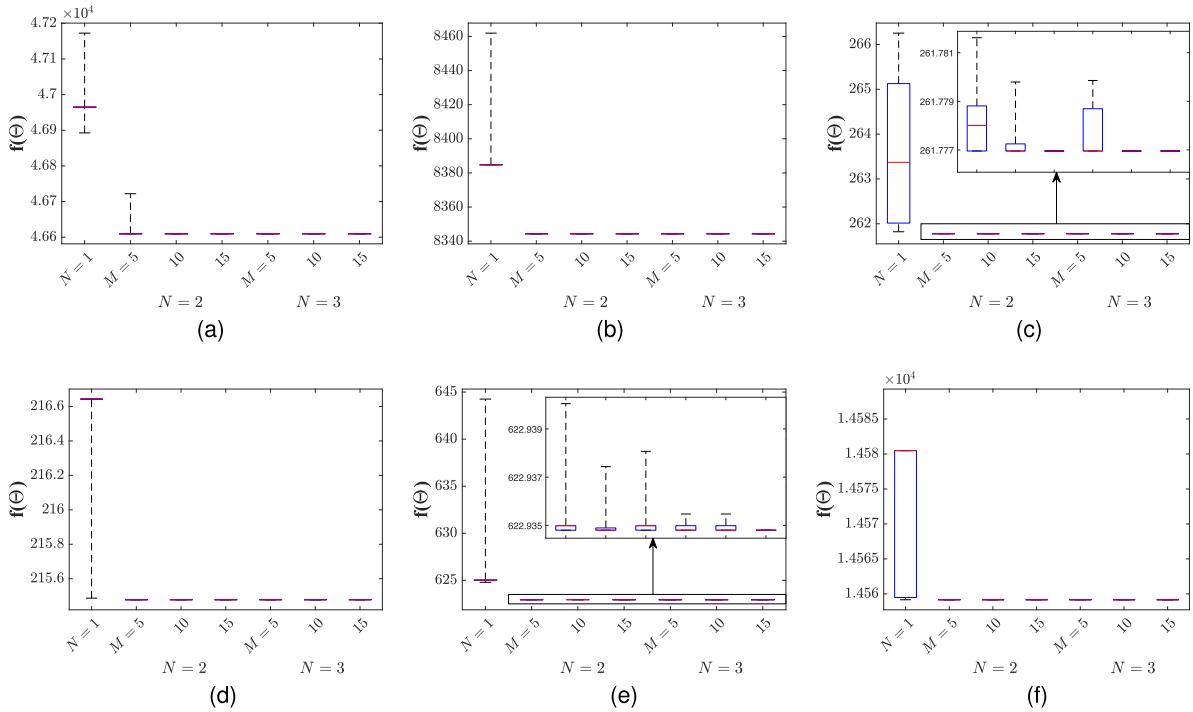

Fig. 4. Monte Carlo test results using CAFCM with several values of N and M on the six datasets. (a) NCI9. (b) WarpPIE10P. (c) WineQuality-White. (d) PageBlock. (e) Texture. (f) Optdigits.

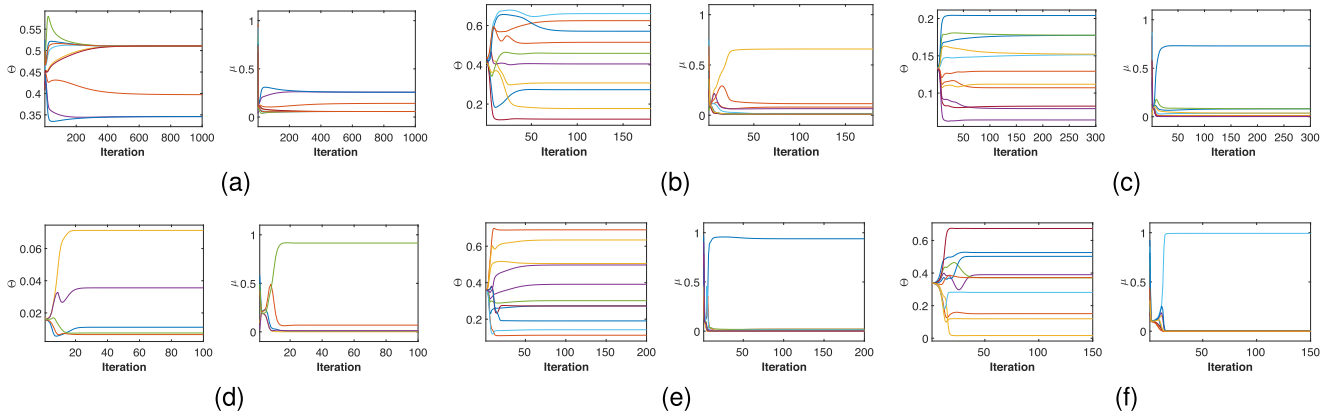

Fig. 5. Snapshots of the convergent centers Θ and the membership degrees μ values in the FCM clustering loop of CAFCM (Steps 6–10) on the six datasets, where the lines in the left-hand side subplots portray the first feature values of k centers, and the lines in the right-hand side subplots portray the k membership degrees. (a) NCI9. (b) WarpPIE10P. (c) WineQuality-White. (d) PageBlock. (e) Texture. (f) Optdigits.

definite, BFC may not be applicable to some datasets. The codes of FSC and MEC are obtained from Github.[16] The codes of KFCM and 2PFCM are shared by the authors of [47] and [54], respectively. The Euclidean distance is used as the dissimilarity measure in all algorithms.

The performance evaluation for the experimental results is based on nineteen internal criteria listed in Table S-I in the Supplementary Materials, and three external criteria described in Section S-I in the Supplementary Materials, Due to the wide range of values of WGSS, CHI, XBI, and TWI, they are normalized by p, $(n-k)/(k-1)$, n, and pk, respectively, to facilitate the later tabular presentation.

Tables II–V tabulate the means and standard deviations of the internal and external cluster validity indices values over 50 runs by using CAFCM and thirteen prevailing algorithms with random initialization on the eight datasets, where $\times$ indicates "not applicable", and the best and second-best results are boldfaced and underlined, respectively. Specifically, CAFCM achieves 81 best and 20 second-best means out of 168 entries (i.e., 48.21% and 60.12% for the best and the best plus the second-best), and CAPKM++2.0 ranks in second place, achieving 40 best and 55 second-best means (i.e., 23.81% and 56.55%), and SC ranks in third place, achieving 23 best and

[16][Online]. Available: https://github.com/kailugaji/Fuzzy_Clustering_Algorithms

TABLE II
MEAN VALUES AND STANDARD DEVIATIONS OF INTERNAL AND EXTERNAL CLUSTER VALIDITY INDICES RESULTING FROM CAFCM, AND THIRTEEN BASELINES ON NCI9 AND WARPPIE10P, WHERE $N = 2$ AND $M = 10$ IN CAPKM++2.0 AND CAFCM ON NCI9, AND $N = 2$ AND $M = 5$ IN CAPKM++2.0 AND CAFCM ON WARPPIE10P

NCI9	KM	KM++	PKM	EWPKM	SC	HC	CAPKM++2.0
WGSS↓	5.2462 ± 0.1468	5.2877 ± 0.1555	4.8592 ± 0.0129	4.8614 ± 0.0114	6.5683 ± 0.1529	5.0366 ± 0.0000	4.8116 ± 0.0029
MRI↓	0.8730 ± 0.0147	0.8734 ± 0.0135	0.8468 ± 0.0056	0.8472 ± 0.0052	1.0039 ± 0.0117	0.8442 ± 0.0000	0.8335 ± 0.0012
GPI↓	0.0488 ± 0.0138	0.0515 ± 0.0149	0.0246 ± 0.0025	0.0247 ± 0.0023	0.2306 ± 0.0263	0.0247 ± 0.0000	0.0183 ± 0.0008
BHGI↑	0.6390 ± 0.0780	0.6386 ± 0.0726	0.7392 ± 0.0340	0.7364 ± 0.0318	-0.0209 ± 0.0584	0.7685 ± 0.0000	0.8268 ± 0.0067
CI↓	0.1656 ± 0.0342	0.1641 ± 0.0319	0.1234 ± 0.0142	0.1246 ± 0.0133	0.5009 ± 0.0347	0.1102 ± 0.0000	0.0866 ± 0.0028
TI↑	0.3300 ± 0.0412	0.3383 ± 0.0420	0.3217 ± 0.0200	0.3195 ± 0.0189	-0.0142 ± 0.0397	0.3551 ± 0.0000	0.3802 ± 0.0040
DGI↑	1.4203 ± 0.0616	1.4370 ± 0.0812	1.5220 ± 0.0197	1.5147 ± 0.0191	1.2395 ± 0.0984	**1.5442 ± 0.0000**	1.4940 ± 0.0216
RLI↑	0.1864 ± 0.0046	0.1883 ± 0.0059	0.1936 ± 0.0006	0.1935 ± 0.0005	0.1218 ± 0.0048	0.1949 ± 0.0000	0.1954 ± 0.0002
CHI↑	0.4874 ± 0.0341	0.5000 ± 0.0418	0.5550 ± 0.0041	0.5543 ± 0.0036	0.1548 ± 0.0140	0.5531 ± 0.0000	0.5704 ± 0.0009
RTI↓	2.1592 ± 0.4266	2.1165 ± 0.5580	1.8350 ± 0.0743	1.8238 ± 0.0725	6.6390 ± 2.6748	1.8860 ± 0.0000	1.4976 ± 0.0811
WGI↑	0.1928 ± 0.0142	0.1938 ± 0.0175	0.2093 ± 0.0047	0.2088 ± 0.0047	0.1237 ± 0.0325	0.2143 ± 0.0000	0.2347 ± 0.0027
DI↑	0.6114 ± 0.0332	0.6227 ± 0.0336	0.6634 ± 0.0089	0.6626 ± 0.0113	0.4727 ± 0.0127	0.6890 ± 0.0000	0.6568 ± 0.0075
BHI↑	718.3157 ± 59.4908	727.5179 ± 55.6430	777.2263 ± 5.3801	778.3961 ± 5.3559	520.9616 ± 150.5932	705.6937 ± 0.0000	760.8223 ± 6.2293
PBMI↑	44.2921 ± 8.8454	47.9437 ± 11.1767	57.0968 ± 2.6056	57.2552 ± 2.3421	48.1918 ± 12.6702	52.3096 ± 0.0000	41.1212 ± 0.1705
XBI↓	0.0120 ± 0.0010	0.0119 ± 0.0011	0.0102 ± 0.0000	0.0102 ± 0.0000	0.0161 ± 0.0006	0.0102 ± 0.0000	0.0101 ± 0.0000
DBI↓	2.3937 ± 0.1579	2.3963 ± 0.1722	2.5070 ± 0.0599	2.5108 ± 0.0578	2.6560 ± 0.5068	2.2793 ± 0.0000	2.2491 ± 0.0248
LSSRI↑	-0.7765 ± 0.0666	-0.8055 ± 0.0865	-0.5888 ± 0.0074	-0.5900 ± 0.0066	-1.8693 ± 0.0870	-0.5921 ± 0.0000	-0.5615 ± 0.0017
TWI↓	0.5749 ± 0.0120	0.5800 ± 0.0154	0.5399 ± 0.0014	0.5401 ± 0.0013	0.7271 ± 0.0087	0.5406 ± 0.0000	0.5346 ± 0.0003
ACC↑	0.3973 ± 0.0417	0.3907 ± 0.0464	0.4373 ± 0.0141	0.4317 ± 0.0144	0.2623 ± 0.0225	**0.4667 ± 0.0000**	0.4640 ± 0.0085
NMI↑	0.3976 ± 0.0440	0.3922 ± 0.0447	0.4753 ± 0.0134	0.4720 ± 0.0140	0.2475 ± 0.0302	0.4750 ± 0.0000	**0.4811 ± 0.0056**
ARI↑	0.1113 ± 0.0412	0.1084 ± 0.0453	0.1773 ± 0.0138	0.1729 ± 0.0147	0.0019 ± 0.0164	0.1946 ± 0.0000	**0.2005 ± 0.0082**

NCI9	FCM	MEC	FSC	2PFCM	BFC	KFCM	CAFCM
WGSS↓	6.4080 ± 0.0000	6.4080 ± 0.0000	6.3000 ± 0.1441	6.4080 ± 0.0000	×	6.2337 ± 0.1136	**4.7992 ± 0.0000**
MRI↓	0.8775 ± 0.0000	0.8775 ± 0.0000	0.9983 ± 0.0087	0.8775 ± 0.0000	×	0.8862 ± 0.0035	**0.8314 ± 0.0000**
GPI↓	0.0872 ± 0.0000	0.0872 ± 0.0000	0.0971 ± 0.0058	0.0872 ± 0.0000	×	0.0988 ± 0.0062	**0.0168 ± 0.0000**
BHGI↑	0.6512 ± 0.0000	0.6512 ± 0.0000	0.0052 ± 0.0433	0.6512 ± 0.0000	×	0.5948 ± 0.0226	**0.8553 ± 0.0000**
CI↓	0.1481 ± 0.0000	0.1481 ± 0.0000	0.4534 ± 0.0187	0.1481 ± 0.0000	×	0.1732 ± 0.0101	**0.0750 ± 0.0000**
TI↑	**0.4606 ± 0.0000**	**0.4606 ± 0.0000**	0.0023 ± 0.0193	**0.4606 ± 0.0000**	×	0.4152 ± 0.0153	0.4128 ± 0.0000
DGI↑	1.5162 ± 0.0000	1.5162 ± 0.0000	1.2437 ± 0.0333	1.5162 ± 0.0000	×	1.4460 ± 0.0692	1.4970 ± 0.0000
RLI↑	**0.2620 ± 0.0000**	**0.2620 ± 0.0000**	0.1231 ± 0.0052	**0.2620 ± 0.0000**	×	0.1976 ± 0.0110	0.1970 ± 0.0000
CHI↑	**1.6299 ± 0.0000**	**1.6299 ± 0.0000**	0.1587 ± 0.0172	**1.6299 ± 0.0000**	×	0.5960 ± 0.0971	0.5744 ± 0.0000
RTI↓	**1.3893 ± 0.0000**	**1.3893 ± 0.0000**	4.9573 ± 0.5891	**1.3893 ± 0.0000**	×	1.5432 ± 0.3750	1.7243 ± 0.0000
WGI↑	0.2265 ± 0.0000	0.2265 ± 0.0000	0.0609 ± 0.0058	0.2265 ± 0.0000	×	0.2348 ± 0.0316	**0.2366 ± 0.0000**
DI↑	0.5961 ± 0.0000	0.5961 ± 0.0000	0.4831 ± 0.0153	0.5961 ± 0.0000	×	0.5718 ± 0.0303	**0.7067 ± 0.0000**
BHI↑	**1031.1357 ± 0.0000**	**1031.1357 ± 0.0000**	1025.6173 ± 26.0115	**1031.1357 ± 0.0000**	×	588.0926 ± 152.9647	695.6437 ± 0.0000
PBMI↑	**220.2380 ± 0.0000**	**220.2380 ± 0.0000**	12.7660 ± 3.7023	**220.2380 ± 0.0000**	×	90.7854 ± 22.4696	46.3868 ± 0.0000
XBI↓	0.0131 ± 0.0000	0.0131 ± 0.0000	0.0163 ± 0.0003	0.0131 ± 0.0000	×	0.0136 ± 0.0013	**0.0101 ± 0.0000**
DBI↓	2.3399 ± 0.0000	2.3399 ± 0.0000	3.9249 ± 0.1331	2.3399 ± 0.0000	×	**1.8879 ± 0.3532**	2.1064 ± 0.0000
LSSRI↑	-1.7195 ± 0.0000	-1.7195 ± 0.0000	-1.8462 ± 0.1079	-1.7195 ± 0.0000	×	-1.4070 ± 0.0860	**-0.5543 ± 0.0000**
TWI↓	0.7120 ± 0.0000	0.7120 ± 0.0000	0.7247 ± 0.0107	0.7120 ± 0.0000	×	0.6741 ± 0.0115	**0.5332 ± 0.0000**
ACC↑	0.2000 ± 0.0000	0.2000 ± 0.0000	0.2960 ± 0.0253	0.2000 ± 0.0000	×	0.2377 ± 0.0146	**0.4667 ± 0.0000**
NMI↑	0.0649 ± 0.0000	0.0649 ± 0.0000	0.2855 ± 0.0335	0.0649 ± 0.0000	×	0.1473 ± 0.0197	0.4553 ± 0.0000
ARI↑	0.0050 ± 0.0000	0.0050 ± 0.0000	0.0007 ± 0.0247	0.0050 ± 0.0000	×	0.0107 ± 0.0055	0.1775 ± 0.0000

WarpPIE10P	KM	KM++	PKM	EWPKM	SC	HC	CAPKM++2.0
WGSS↓	3.6702 ± 0.1250	3.6396 ± 0.1102	3.4673 ± 0.0081	3.4660 ± 0.0053	5.4244 ± 0.1375	3.5330 ± 0.0000	3.4485 ± 0.0007
MRI↓	0.5617 ± 0.0153	0.5549 ± 0.0114	0.5519 ± 0.0020	0.5528 ± 0.0011	1.0070 ± 0.0072	0.5548 ± 0.0000	0.5375 ± 0.0014
GPI↓	0.0184 ± 0.0038	0.0168 ± 0.0025	0.0152 ± 0.0003	0.0154 ± 0.0001	0.2305 ± 0.0077	0.0168 ± 0.0000	0.0132 ± 0.0002
BHGI↑	0.8269 ± 0.0287	0.8398 ± 0.0231	0.8334 ± 0.0030	0.8314 ± 0.0021	-0.0002 ± 0.0140	0.8260 ± 0.0000	0.8589 ± 0.0012
CI↓	0.0924 ± 0.0127	0.0867 ± 0.0113	0.0938 ± 0.0014	0.0945 ± 0.0012	0.4955 ± 0.0101	0.0925 ± 0.0000	0.0793 ± 0.0008
TI↑	0.3804 ± 0.0204	0.3849 ± 0.0232	0.3555 ± 0.0005	0.3550 ± 0.0015	-0.0002 ± 0.0097	0.3630 ± 0.0000	0.3715 ± 0.0009
DGI↑	0.4522 ± 0.0789	0.4596 ± 0.0865	0.4318 ± 0.0280	0.4442 ± 0.0285	**0.6521 ± 0.0102**	0.6178 ± 0.0000	0.6017 ± 0.0483
RLI↑	0.2544 ± 0.0030	0.2548 ± 0.0019	0.2575 ± 0.0002	0.2575 ± 0.0001	0.1493 ± 0.0052	0.2550 ± 0.0000	0.2576 ± 0.0002
CHI↑	2.0035 ± 0.1020	2.0236 ± 0.0852	2.1704 ± 0.0073	2.1717 ± 0.0048	0.3086 ± 0.0273	2.0299 ± 0.0000	2.1877 ± 0.0006
RTI↓	1.1935 ± 0.3724	1.0997 ± 0.1915	0.9863 ± 0.0381	0.9807 ± 0.0281	3.2132 ± 0.6500	**0.9082 ± 0.0000**	0.9109 ± 0.0115
WGI↑	0.3000 ± 0.0166	0.3023 ± 0.0167	0.3032 ± 0.0016	0.3035 ± 0.0013	0.1608 ± 0.0138	0.3058 ± 0.0000	0.3275 ± 0.0046
DI↑	0.1508 ± 0.0278	0.1571 ± 0.0299	0.1619 ± 0.0106	0.1662 ± 0.0079	0.1653 ± 0.0000	0.2062 ± 0.0000	0.2284 ± 0.0188
BHI↑	41.1859 ± 1.4855	41.8175 ± 1.4292	39.6807 ± 0.5807	39.4854 ± 0.3599	29.1643 ± 1.4002	42.0479 ± 0.0000	41.2249 ± 0.0376
PBMI↑	14.8197 ± 1.7981	15.7846 ± 1.8157	15.4603 ± 0.1819	15.2328 ± 0.0447	7.4846 ± 0.2832	15.1854 ± 0.0000	15.2649 ± 0.1076
XBI↓	0.0322 ± 0.0136	0.0311 ± 0.0116	0.0301 ± 0.0061	0.0281 ± 0.0020	0.0161 ± 0.0004	0.0146 ± 0.0000	0.0156 ± 0.0036
DBI↓	1.6531 ± 0.0813	1.6543 ± 0.0833	1.5892 ± 0.0337	1.5787 ± 0.0106	1.6824 ± 0.0650	1.5338 ± 0.0000	1.5912 ± 0.0216
LSSRI↑	0.6911 ± 0.0509	0.7040 ± 0.0432	0.7749 ± 0.0034	0.7755 ± 0.0022	-1.1803 ± 0.1009	0.7080 ± 0.0000	0.7829 ± 0.0003
TWI↓	0.3670 ± 0.0125	0.3639 ± 0.0106	0.3467 ± 0.0008	0.3466 ± 0.0005	0.8404 ± 0.0185	0.3628 ± 0.0000	0.3448 ± 0.0001
ACC↑	0.2808 ± 0.0238	0.2849 ± 0.0223	0.2726 ± 0.0043	0.2720 ± 0.0042	**0.2874 ± 0.0136**	0.2857 ± 0.0000	0.2827 ± 0.0037
NMI↑	0.3006 ± 0.0334	0.3024 ± 0.0304	0.3062 ± 0.0037	0.3140 ± 0.0054	**0.3835 ± 0.0155**	0.3614 ± 0.0000	0.3112 ± 0.0051
ARI↑	0.0872 ± 0.0209	0.0893 ± 0.0204	0.0927 ± 0.0040	0.0962 ± 0.0044	0.0917 ± 0.0162	**0.1117 ± 0.0000**	0.0932 ± 0.0017

WarpPIE10P	FCM	MEC	FSC	2PFCM	BFC	KFCM	CAFCM
WGSS↓	4.0995 ± 0.0781	5.7692 ± 0.4605	4.5079 ± 0.2281	4.1417 ± 0.0000	×	4.9026 ± 0.3384	**3.4481 ± 0.0000**
MRI↓	0.5964 ± 0.0033	0.6727 ± 0.0235	0.6437 ± 0.0320	0.5966 ± 0.0000	×	0.6351 ± 0.0209	**0.5368 ± 0.0000**
GPI↓	0.0265 ± 0.0012	0.0730 ± 0.0137	0.0457 ± 0.0130	0.0267 ± 0.0000	×	0.0506 ± 0.0119	**0.0131 ± 0.0000**
BHGI↑	0.7720 ± 0.0045	0.6944 ± 0.0510	0.6857 ± 0.0667	0.7723 ± 0.0000	×	0.7501 ± 0.0406	**0.8594 ± 0.0000**
CI↓	0.1181 ± 0.0020	0.1350 ± 0.0258	0.1488 ± 0.0297	0.1176 ± 0.0000	×	0.1118 ± 0.0185	**0.0788 ± 0.0000**
TI↑	0.3719 ± 0.0054	**0.4790 ± 0.0341**	0.3676 ± 0.0401	0.3739 ± 0.0000	×	0.4743 ± 0.0371	0.3712 ± 0.0000
DGI↑	0.3726 ± 0.0150	0.4923 ± 0.1518	0.3584 ± 0.0614	0.3753 ± 0.0000	×	0.4407 ± 0.0981	0.6128 ± 0.0000
RLI↑	0.2672 ± 0.0069	**0.3029 ± 0.0253**	0.2321 ± 0.0095	0.2737 ± 0.0000	×	0.2742 ± 0.0215	0.2575 ± 0.0000
CHI↑	1.9728 ± 0.1043	2.0753 ± 0.4907	1.2087 ± 0.1801	2.0772 ± 0.0000	×	1.7966 ± 0.3492	**2.1881 ± 0.0000**
RTI↓	1.8281 ± 0.1085	1.1546 ± 0.6850	2.9239 ± 1.1012	1.8725 ± 0.0000	×	2.2566 ± 1.4066	0.9166 ± 0.0000
WGI↑	0.2094 ± 0.0058	0.2998 ± 0.0599	0.1626 ± 0.0444	0.2108 ± 0.0000	×	0.2580 ± 0.0438	**0.3298 ± 0.0000**
DI↑	0.1200 ± 0.0055	0.1152 ± 0.0347	0.1021 ± 0.0166	0.1216 ± 0.0000	×	0.1179 ± 0.0261	**0.2357 ± 0.0000**
BHI↑	47.7023 ± 1.7305	**56.2621 ± 8.4753**	56.0150 ± 5.3085	49.0781 ± 0.0000	×	44.7456 ± 6.3442	41.2083 ± 0.0000
PBMI↑	18.3786 ± 1.6131	**35.9067 ± 10.626**	8.6801 ± 1.8138	18.6328 ± 0.0000	×	15.8542 ± 4.2921	15.2014 ± 0.0000
XBI↓	0.0454 ± 0.0056	0.0478 ± 0.0260	0.0513 ± 0.0168	0.0446 ± 0.0000	×	0.0459 ± 0.0199	**0.0143 ± 0.0000**
DBI↓	2.0949 ± 0.0706	**1.4158 ± 0.2782**	2.4521 ± 0.2813	2.1304 ± 0.0000	×	1.6098 ± 0.3075	1.6021 ± 0.0000
LSSRI↑	0.4750 ± 0.0242	-0.3174 ± 0.2081	0.1485 ± 0.1483	0.4698 ± 0.0000	×	0.0836 ± 0.1595	**0.7830 ± 0.0000**
TWI↓	0.4215 ± 0.0063	0.6353 ± 0.0555	0.5091 ± 0.0404	0.4229 ± 0.0000	×	0.5268 ± 0.0434	**0.3448 ± 0.0000**
ACC↑	0.1991 ± 0.0045	0.1373 ± 0.0164	0.2636 ± 0.0281	0.2000 ± 0.0000	×	0.1675 ± 0.0196	0.2810 ± 0.0000
NMI↑	0.1378 ± 0.0103	0.0587 ± 0.0249	0.2673 ± 0.0445	0.1336 ± 0.0000	×	0.1084 ± 0.0325	0.3140 ± 0.0000
ARI↑	0.0264 ± 0.0031	-0.0034 ± 0.0059	0.0591 ± 0.0254	0.0250 ± 0.0000	×	0.0058 ± 0.0097	0.0940 ± 0.0000

The best ones are boldfaced and second best ones are underlined.

TABLE III
MEAN VALUES AND STANDARD DEVIATIONS OF INTERNAL AND EXTERNAL CLUSTER VALIDITY INDICES RESULTING FROM CAFCM, AND THIRTEEN BASELINES ON WQ-WHITE AND PAGEBLOCKS, WHERE $N = 2$ AND $M = 15$ IN CAPKM++2.0 AND CAFCM ON WQ-WHITE, AND $N = 2$ AND $M = 5$ IN CAPKM++2.0 AND CAFCM ON PAGEBLOCKS

WQ-White	KM	KM++	PKM	EWPKM	SC	HC	CAPKM++2.0
WGSS↓	24.1112 ± 0.2265	24.0518 ± 0.2140	24.1402 ± 0.0557	31.1401 ± 0.5426	26.7792 ± 0.5784	24.7211 ± 0.0000	23.7983 ± 0.0003
MRI↓	0.6234 ± 0.0049	0.6210 ± 0.0041	0.6218 ± 0.0023	0.7862 ± 0.0086	0.6990 ± 0.0118	0.6672 ± 0.0000	0.6134 ± 0.0003
GPI↓	0.0268 ± 0.0011	0.0266 ± 0.0010	0.0261 ± 0.0004	0.0568 ± 0.0010	0.0684 ± 0.0094	0.0409 ± 0.0000	0.0259 ± 0.0001
BHGI↑	0.7087 ± 0.0111	0.7137 ± 0.0095	0.7091 ± 0.0044	0.3820 ± 0.0164	0.5778 ± 0.0217	0.6272 ± 0.0000	0.7315 ± 0.0007
CI↓	0.1318 ± 0.0048	0.1295 ± 0.0041	0.1314 ± 0.0019	0.2658 ± 0.0070	0.1825 ± 0.0103	0.1638 ± 0.0000	0.1218 ± 0.0003
TI↑	0.3042 ± 0.0100	0.3077 ± 0.0090	0.3002 ± 0.0021	0.1639 ± 0.0082	0.3277 ± 0.0061	0.2939 ± 0.0000	0.3213 ± 0.0003
DGI↑	0.0985 ± 0.0304	0.0925 ± 0.0236	0.0857 ± 0.0294	0.0788 ± 0.0117	0.0724 ± 0.0287	**0.3741 ± 0.0000**	0.0897 ± 0.0177
RLI↑	0.1982 ± 0.0045	0.1991 ± 0.0040	0.1936 ± 0.0005	0.1918 ± 0.0043	0.1873 ± 0.0032	0.1921 ± 0.0000	**0.2020 ± 0.0001**
CHI↑	1.2958 ± 0.0215	1.3019 ± 0.0189	1.2927 ± 0.0054	0.5167 ± 0.0211	0.9218 ± 0.0532	1.0443 ± 0.0000	1.3258 ± 0.0000
RTI↓	1.2338 ± 0.1081	1.2356 ± 0.1258	1.2730 ± 0.0420	4.6374 ± 0.6606	1.7116 ± 0.6944	1.4968 ± 0.0000	**1.0232 ± 0.0355**
WGI↑	0.2339 ± 0.0061	0.2358 ± 0.0052	0.2313 ± 0.0012	0.0372 ± 0.0044	0.2095 ± 0.0123	0.1669 ± 0.0000	**0.2432 ± 0.0001**
DI↑	0.0107 ± 0.0032	0.0105 ± 0.0027	0.0101 ± 0.0029	0.0105 ± 0.0015	0.0079 ± 0.0031	**0.0389 ± 0.0000**	0.0108 ± 0.0021
BHI↑	0.0580 ± 0.0017	0.0581 ± 0.0010	0.0577 ± 0.0004	0.0822 ± 0.0007	0.0501 ± 0.0017	0.0642 ± 0.0000	0.0593 ± 0.0001
PBMI↑	0.0090 ± 0.0008	0.0097 ± 0.0051	0.0088 ± 0.0003	0.0043 ± 0.0001	**0.0187 ± 0.0005**	0.0077 ± 0.0000	0.0089 ± 0.0000
XBI↓	0.0441 ± 0.0538	0.0411 ± 0.0283	0.0601 ± 0.0726	0.0662 ± 0.0277	0.1812 ± 0.4440	**0.0022 ± 0.0000**	0.0385 ± 0.0076
DBI↓	1.7215 ± 0.0582	1.7092 ± 0.0605	1.7443 ± 0.0134	3.3640 ± 0.2439	**1.5007 ± 0.0831**	1.8248 ± 0.0000	1.6309 ± 0.0040
LSSRI↑	0.2590 ± 0.0166	0.2637 ± 0.0146	0.2567 ± 0.0042	-0.6611 ± 0.0406	-0.0832 ± 0.0609	0.0433 ± 0.0000	**0.2820 ± 0.0000**
TWI↓	2.1919 ± 0.0206	2.1860 ± 0.0181	2.1947 ± 0.0052	3.3182 ± 0.0459	2.6203 ± 0.0762	2.4613 ± 0.0000	2.1635 ± 0.0000
ACC↑	0.1911 ± 0.0110	0.1943 ± 0.0110	0.1883 ± 0.0028	0.1778 ± 0.0082	0.3136 ± 0.0223	0.2201 ± 0.0000	0.2034 ± 0.0009
NMI↑	0.0828 ± 0.0026	0.0825 ± 0.0022	0.0833 ± 0.0012	0.0531 ± 0.0045	0.0762 ± 0.0042	0.0695 ± 0.0000	0.0809 ± 0.0004
ARI↑	0.0314 ± 0.0014	0.0315 ± 0.0014	0.0314 ± 0.0007	0.0173 ± 0.0018	0.0411 ± 0.0038	0.0315 ± 0.0000	0.0314 ± 0.0002

WQ-White	FCM	MEC	FSC	2PFCM	BFC	KFCM	CAFCM
WGSS↓	30.3011 ± 0.2196	30.5183 ± 1.0614	34.1901 ± 0.8792	30.5788 ± 0.0000	39.0307 ± 0.8555	29.1012 ± 0.9733	**23.7979 ± 0.0000**
MRI↓	0.7324 ± 0.0012	0.7389 ± 0.0080	0.9225 ± 0.0082	0.7323 ± 0.0000	0.9606 ± 0.0060	0.7322 ± 0.0125	**0.6130 ± 0.0000**
GPI↓	0.0651 ± 0.0031	0.1110 ± 0.0097	0.0857 ± 0.0044	0.0661 ± 0.0000	0.0773 ± 0.0011	0.0954 ± 0.0121	**0.0258 ± 0.0000**
BHGI↑	0.5026 ± 0.0019	0.5192 ± 0.0151	0.1354 ± 0.0146	0.5032 ± 0.0000	0.0703 ± 0.0113	0.5217 ± 0.0268	**0.7323 ± 0.0000**
CI↓	0.2174 ± 0.0009	0.2180 ± 0.0087	0.3760 ± 0.0068	0.2171 ± 0.0000	0.4016 ± 0.0047	0.2114 ± 0.0127	**0.1215 ± 0.0000**
TI↑	0.2570 ± 0.0064	**0.3524 ± 0.0166**	0.0603 ± 0.0063	0.2597 ± 0.0000	0.0287 ± 0.0046	0.3291 ± 0.0264	0.3216 ± 0.0000
DGI↑	0.0447 ± 0.0271	0.0844 ± 0.0662	0.0476 ± 0.0099	0.0565 ± 0.0000	0.0000± 0.0000	0.0914 ± 0.0583	0.1489 ± 0.0000
RLI↑	0.1589 ± 0.0023	0.1589 ± 0.0109	0.1106 ± 0.0077	0.1658 ± 0.0000	0.0660 ± 0.0049	0.1616 ± 0.0071	0.2019 ± 0.0000
CHI↑	0.6882 ± 0.0227	0.6668 ± 0.1235	0.1728 ± 0.0301	0.7568 ± 0.0000	0.0724 ± 0.0118	0.7021 ± 0.0790	**1.3258 ± 0.0000**
RTI↓	28.4805 ± 11.1635	6.2702 ± 4.4866	61.0821 ± 18.5534	31.9810 ± 0.0000	303.0457 ± 124.7866	3.4390 ± 1.3883	1.0290 ± 0.0000
WGI↑	0.0526 ± 0.0040	0.0678 ± 0.0339	0.0069 ± 0.0041	0.0602 ± 0.0000	0.0005 ± 0.0020	0.0838 ± 0.0228	0.2430 ± 0.0000
DI↑	0.0046 ± 0.0027	0.0089 ± 0.0070	0.0067 ± 0.0014	0.0066 ± 0.0000	0.0000± 0.0000	0.0100 ± 0.0064	0.0179 ± 0.0000
BHI↑	0.0698 ± 0.0036	0.0561 ± 0.0065	0.1028 ± 0.0043	0.0757 ± 0.0000	**0.1159 ± 0.0014**	0.0590 ± 0.0054	0.0593 ± 0.0000
PBMI↑	0.0055 ± 0.0004	0.0056 ± 0.0026	0.0026 ± 0.0006	0.0065 ± 0.0000	0.0007 ± 0.0002	0.0037 ± 0.0014	0.0089 ± 0.0000
XBI↓	0.5431 ± 0.7058	0.7697 ± 1.0280	0.1935 ± 0.0874	0.0947 ± 0.0000	∞ ± NaN	0.2875 ± 0.5703	0.0131 ± 0.0000
DBI↓	5.9397 ± 0.6268	2.3661 ± 0.3880	9.5955 ± 0.9188	5.8677 ± 0.0000	22.1934 ± 3.0747	2.2232 ± 0.1841	1.6294 ± 0.0000
LSSRI↑	-0.3826 ± 0.0090	-0.6364 ± 0.1396	-1.7714 ± 0.1821	-0.3843 ± 0.0000	-2.6392 ± 0.1691	-0.4159 ± 0.1070	**0.2820 ± 0.0000**
TWI↓	2.9913 ± 0.0109	3.2871 ± 0.1599	4.2932 ± 0.1104	2.9934 ± 0.0000	4.6927 ± 0.0516	3.0302 ± 0.1278	**2.1634 ± 0.0000**
ACC↑	0.2750 ± 0.0082	**0.4071 ± 0.0319**	0.1794 ± 0.0078	0.2799 ± 0.0000	0.1216 ± 0.0034	0.3585 ± 0.0366	0.2023 ± 0.0000
NMI↑	0.0791 ± 0.0006	**0.0843 ± 0.0064**	0.0302 ± 0.0036	0.0796 ± 0.0000	0.0144 ± 0.0016	0.0789 ± 0.0053	0.0806 ± 0.0000
ARI↑	0.0452 ± 0.0023	**0.0697 ± 0.0108**	0.0098 ± 0.0016	0.0464 ± 0.0000	0.0042 ± 0.0008	0.0597 ± 0.0136	0.0311 ± 0.0000

PageBlocks	KM	KM++	PKM	EWPKM	SC	HC	CAPKM++2.0
WGSS↓	21.7169 ± 0.3282	22.1370 ± 0.6964	21.6463 ± 0.0431	38.1295 ± 0.0053	24.9753 ± 0.0000	22.5422 ± 0.0000	**21.5478 ± 0.0000**
MRI↓	0.4072 ± 0.0058	0.4087 ± 0.0072	0.4080 ± 0.0046	0.5264 ± 0.0001	0.4738 ± 0.0000	0.4167 ± 0.0000	0.3974 ± 0.0001
GPI↓	0.0504 ± 0.0019	0.0517 ± 0.0033	0.0504 ± 0.0012	0.0892 ± 0.0001	0.0797 ± 0.0000	0.0547 ± 0.0000	0.0476 ± 0.0000
BHGI↑	0.7577 ± 0.0172	0.7617 ± 0.0154	0.7533 ± 0.0144	0.6198 ± 0.0003	0.6547 ± 0.0000	0.7583 ± 0.0000	0.7867 ± 0.0002
CI↓	0.0840 ± 0.0055	0.0840 ± 0.0055	0.0852 ± 0.0046	0.2051 ± 0.0001	0.1327 ± 0.0000	0.0889 ± 0.0000	0.0745 ± 0.0001
TI↑	0.4893 ± 0.0231	0.5023 ± 0.0221	0.4821 ± 0.0186	0.4247 ± 0.0002	0.4450 ± 0.0000	0.5102 ± 0.0000	0.5253 ± 0.0002
DGI↑	0.0243 ± 0.0068	0.0247 ± 0.0068	0.0247 ± 0.0036	0.0098 ± 0.0000	0.0096 ± 0.0000	**0.0610 ± 0.0000**	0.0327 ± 0.0000
RLI↑	0.2586 ± 0.0086	0.2711 ± 0.021	0.2565 ± 0.0025	**0.3121 ± 0.0000**	0.2491 ± 0.0000	0.2541 ± 0.0000	0.2622 ± 0.0000
CHI↑	2.0879 ± 0.0443	2.0315 ± 0.0937	2.0973 ± 0.0062	0.5680 ± 0.0003	1.3952 ± 0.0000	1.8244 ± 0.0000	2.1114 ± 0.0000
RTI↓	0.6878 ± 0.1753	0.5812 ± 0.1759	0.7428 ± 0.1425	0.7824 ± 0.0029	1.4506 ± 0.0000	0.5442 ± 0.0000	0.4168 ± 0.0003
WGI↑	0.4604 ± 0.0249	0.4785 ± 0.0275	0.4523 ± 0.0197	0.4316 ± 0.0002	0.4250 ± 0.0000	0.4269 ± 0.0000	0.4976 ± 0.0001
DI↑	0.0025 ± 0.0008	0.0034 ± 0.0012	0.0025 ± 0.0004	0.0025 ± 0.0000	0.0010 ± 0.0000	**0.0067 ± 0.0000**	0.0034 ± 0.0000
BHI↑	0.0617 ± 0.0125	0.0794 ± 0.0275	0.0582 ± 0.0041	**0.2173 ± 0.0000**	0.0554 ± 0.0000	0.0586 ± 0.0000	0.0678 ± 0.0000
PBMI↑	0.1118 ± 0.0137	**0.1583 ± 0.0829**	0.1090 ± 0.0100	0.0926 ± 0.0000	0.1108 ± 0.0000	0.1062 ± 0.0000	0.1324 ± 0.0000
XBI↓	0.3369 ± 0.1914	0.2285 ± 0.1610	0.2881 ± 0.0746	0.6293 ± 0.0001	1.7756 ± 0.0000	**0.0478 ± 0.0000**	0.1190 ± 0.0000
DBI↓	1.0248 ± 0.0060	**0.9943 ± 0.0669**	1.0267 ± 0.0021	1.5361 ± 0.0021	1.0918 ± 0.0000	1.0082 ± 0.0000	1.0207 ± 0.0000
LSSRI↑	0.7359 ± 0.0221	0.7077 ± 0.0468	0.7406 ± 0.0029	-0.5657 ± 0.0006	0.3331 ± 0.0000	0.6013 ± 0.0000	**0.7474 ± 0.0000**
TWI↓	4.3434 ± 0.0656	4.4274 ± 0.1393	4.3293 ± 0.0086	8.5517 ± 0.0019	5.5982 ± 0.0000	4.7475 ± 0.0000	4.3096 ± 0.0000
ACC↑	0.4416 ± 0.0588	0.4822 ± 0.0625	0.4222 ± 0.0463	0.7193 ± 0.0001	0.4793 ± 0.0000	0.5387 ± 0.0000	0.5291 ± 0.0004
NMI↑	0.1529 ± 0.0039	0.1545 ± 0.0050	0.1514 ± 0.0007	0.1003 ± 0.0000	0.1737 ± 0.0000	0.1578 ± 0.0000	0.1505 ± 0.0001
ARI↑	0.0952 ± 0.0096	0.1029 ± 0.0110	0.0914 ± 0.0067	0.0528 ± 0.0001	0.0866 ± 0.0000	0.1226 ± 0.0000	0.1077 ± 0.0002

PageBlocks	FCM	MEC	FSC	2PFCM	BFC	KFCM	CAFCM
WGSS↓	21.8530 ± 0.0000	34.2909 ± 2.9662	41.3223 ± 1.1842	21.8530 ± 0.0000	52.5699 ± 4.7438	31.4679 ± 2.8910	**21.5478 ± 0.0000**
MRI↓	0.4232 ± 0.0000	0.6254 ± 0.0476	0.5970 ± 0.0128	0.4232 ± 0.0000	0.9579 ± 0.0301	0.6010 ± 0.0541	**0.3973 ± 0.0000**
GPI↓	0.0532 ± 0.0000	0.1318 ± 0.0150	0.1031 ± 0.0095	0.0532 ± 0.0000	0.1557 ± 0.0040	0.1161 ± 0.0184	**0.0475 ± 0.0000**
BHGI↑	0.7142 ± 0.0000	0.4501 ± 0.0669	0.5007 ± 0.0268	0.7142 ± 0.0000	0.0441 ± 0.0308	0.4788 ± 0.0757	**0.7871 ± 0.0000**
CI↓	0.0976 ± 0.0000	0.2499 ± 0.0330	0.2945 ± 0.0085	0.0976 ± 0.0000	0.3822 ± 0.0124	0.2203 ± 0.0370	**0.0744 ± 0.0000**
TI↑	0.4356 ± 0.0000	0.3122 ± 0.0487	0.3210 ± 0.0123	0.4356 ± 0.0000	0.0253 ± 0.0179	0.3196 ± 0.0523	**0.5257 ± 0.0000**
DGI↑	0.0342 ± 0.0000	0.0219 ± 0.0061	0.0010 ± 0.0001	0.0342 ± 0.0000	0.0000± 0.0000	0.0220 ± 0.0060	0.0327 ± 0.0000
RLI↑	0.2544 ± 0.0000	0.1994 ± 0.0177	0.1406 ± 0.0090	0.2544 ± 0.0000	0.0645 ± 0.0235	0.2085 ± 0.0155	0.2622 ± 0.0000
CHI↑	2.0556 ± 0.0000	0.7092 ± 0.1532	0.1743 ± 0.0122	2.0556 ± 0.0000	0.0407 ± 0.0311	0.8305 ± 0.1698	**2.1114 ± 0.0000**
RTI↓	1.1244 ± 0.0000	4.4488 ± 7.6595	4.6271 ± 1.2316	1.1244 ± 0.0000	1549.5546 ± 1722.8200	2.3455 ± 1.8063	**0.4160 ± 0.0000**
WGI↑	0.4171 ± 0.0000	0.1496 ± 0.1103	0.1145 ± 0.1211	0.4171 ± 0.0000	0.0031 ± 0.0075	0.1767 ± 0.0886	**0.4978 ± 0.0000**
DI↑	0.0034 ± 0.0000	0.0023 ± 0.0006	0.0002 ± 0.0000	0.0034 ± 0.0000	0.0000± 0.0000	0.0023 ± 0.0007	0.0034 ± 0.0000
BHI↑	0.0552 ± 0.0000	0.0681 ± 0.0190	0.1957 ± 0.0211	0.0552 ± 0.0000	0.1204 ± 0.0021	0.0655 ± 0.0134	0.0678 ± 0.0000
PBMI↑	0.1047 ± 0.0000	0.0202 ± 0.0061	0.0223 ± 0.0080	0.1047 ± 0.0000	0.0024 ± 0.0041	0.0249 ± 0.0082	0.1323 ± 0.0000
XBI↓	0.1466 ± 0.0000	1.3735 ± 5.1380	139.8571 ± 9.2299	0.1466 ± 0.0000	∞ ± NaN	0.6332 ± 0.4108	0.1190 ± 0.0000
DBI↓	1.1062 ± 0.0000	1.6489 ± 0.5322	3.5630 ± 0.4570	1.1062 ± 0.0000	33.3310 ± 13.4587	1.4613 ± 0.2929	1.0206 ± 0.0000
LSSRI↑	0.7206 ± 0.0000	-0.4349 ± 0.2160	-1.7495 ± 0.0680	0.7206 ± 0.0000	-3.4776 ± 0.8038	-0.2110 ± 0.1899	**0.7474 ± 0.0000**
TWI↓	4.3883 ± 0.0000	8.1256 ± 0.6950	11.4202 ± 0.1176	4.3883 ± 0.0000	12.8945 ± 0.3714	7.4034 ± 0.6250	**4.3096 ± 0.0000**
ACC↑	0.3575 ± 0.0000	0.4894 ± 0.0505	**0.8457 ± 0.0116**	0.3575 ± 0.0000	0.2314 ± 0.0170	0.4434 ± 0.0549	0.5302 ± 0.0000
NMI↑	0.1401 ± 0.0000	0.0415 ± 0.0131	**0.2585 ± 0.0113**	0.1401 ± 0.0000	0.0046 ± 0.0052	0.0598 ± 0.0254	0.1506 ± 0.0000
ARI↑	0.0639 ± 0.0000	-0.0006 ± 0.0173	**0.4696 ± 0.0232**	0.0639 ± 0.0000	0.0011 ± 0.0018	0.0120 ± 0.0295	0.1081 ± 0.0000

The best ones are boldfaced and second best ones are underlined.

TABLE IV
MEAN VALUES AND STANDARD DEVIATIONS OF INTERNAL AND EXTERNAL CLUSTER VALIDITY INDICES RESULTING FROM CAFCM, AND THIRTEEN BASELINES ON TEXTURE AND OPTDIGITS, WHERE $N = 3$ AND $M = 15$ IN CAPKM++2.0 AND CAFCM ON TEXTURE, AND $N = 2$ AND $M = 5$ IN CAPKM++2.0 AND CAFCM ON OPTDIGITS

Texture	KM	KM++	PKM	EWPKM	SC	HC	CAPKM++2.0
WGSS↓	16.3911 ± 1.0559	15.9094 ± 0.6088	15.6292 ± 0.0044	15.6776 ± 0.0029	19.2342 ± 0.4501	16.1971 ± 0.0000	15.5736 ± 0.0004
MRI↓	0.3433 ± 0.0135	0.3375 ± 0.0085	0.3337 ± 0.0003	0.3345 ± 0.0001	0.4125 ± 0.0172	0.3535 ± 0.0000	0.3332 ± 0.0003
GPI↓	0.0097 ± 0.0022	0.0087 ± 0.0014	0.0081 ± 0.0000	0.0082 ± 0.0000	0.0246 ± 0.0054	0.0115 ± 0.0000	**0.0079 ± 0.0000**
BHGI↑	0.8995 ± 0.0186	0.9092 ± 0.0128	0.9139 ± 0.0002	0.9136 ± 0.0001	0.7962 ± 0.0262	0.8921 ± 0.0000	**0.9199 ± 0.0002**
CI↓	0.0373 ± 0.0064	0.0338 ± 0.0045	0.0323 ± 0.0001	0.0326 ± 0.0000	0.0709 ± 0.0098	0.0389 ± 0.0000	**0.0300 ± 0.0001**
TI↑	0.3940 ± 0.0138	0.3986 ± 0.0126	0.3970 ± 0.0008	0.3977 ± 0.0002	0.3895 ± 0.0052	0.4127 ± 0.0000	0.4095 ± 0.0005
DGI↑	0.1157 ± 0.0175	0.1173 ± 0.0210	0.0996 ± 0.0194	0.1064 ± 0.0001	0.1294 ± 0.0043	**0.2607 ± 0.0000**	0.1067 ± 0.0288
RLI↑	0.2777 ± 0.0023	0.2787 ± 0.0013	0.2793 ± 0.0000	0.2795 ± 0.0000	0.2702 ± 0.0025	0.2764 ± 0.0000	0.2793 ± 0.0000
CHI↑	7.0583 ± 0.4753	7.2822 ± 0.2871	7.4197 ± 0.0024	7.3306 ± 0.0022	5.0688 ± 0.3170	6.5713 ± 0.0000	7.4498 ± 0.0002
RTI↓	1.0800 ± 0.5900	0.8433 ± 0.2548	0.7606 ± 0.0477	0.6440 ± 0.0070	2.2327 ± 0.2134	0.8343 ± 0.0000	0.6207 ± 0.0091
WGI↑	0.4006 ± 0.0169	0.4075 ± 0.0119	0.4072 ± 0.0009	0.4007 ± 0.0003	0.3109 ± 0.0107	0.3707 ± 0.0000	**0.4125 ± 0.0005**
DI↑	0.0178 ± 0.0036	0.0201 ± 0.0043	0.0190 ± 0.0032	0.0199 ± 0.0000	0.0164 ± 0.0011	**0.0464 ± 0.0000**	0.0187 ± 0.0050
BHI↑	0.1312 ± 0.0082	0.1371 ± 0.0073	0.1421 ± 0.0024	0.1405 ± 0.0001	0.1340 ± 0.0034	0.1500 ± 0.0000	0.1391 ± 0.0003
PBMI↑	0.5566 ± 0.0672	0.6295 ± 0.0808	0.7082 ± 0.0197	0.6900 ± 0.0008	0.3830 ± 0.0112	**0.7264 ± 0.0000**	0.6281 ± 0.0032
XBI↓	0.0105 ± 0.0034	0.0097 ± 0.0036	0.0118 ± 0.0036	0.0094 ± 0.0000	0.0119 ± 0.0012	**0.0022 ± 0.0000**	0.0123 ± 0.0045
DBI↓	1.2223 ± 0.0549	1.1994 ± 0.0333	1.1962 ± 0.0109	1.1921 ± 0.0021	1.4880 ± 0.0449	1.2158 ± 0.0000	**1.1751 ± 0.0016**
LSSRI↑	1.9518 ± 0.0709	1.9846 ± 0.0417	2.0041 ± 0.0003	1.9921 ± 0.0003	1.6207 ± 0.0742	1.8827 ± 0.0000	**2.0082 ± 0.0000**
TWI↓	1.4901 ± 0.0960	1.4463 ± 0.0553	1.4208 ± 0.0004	1.4360 ± 0.0004	1.9782 ± 0.1374	1.5801 ± 0.0000	1.4158 ± 0.0000
ACC↑	0.5837 ± 0.0605	0.5955 ± 0.0470	0.6072 ± 0.0145	0.5610 ± 0.0005	**0.6464 ± 0.0093**	0.6258 ± 0.0000	0.5706 ± 0.0010
NMI↑	0.6298 ± 0.0216	0.6342 ± 0.0157	0.6294 ± 0.0006	0.6057 ± 0.0011	**0.7588 ± 0.0102**	0.6666 ± 0.0000	0.6313 ± 0.0006
ARI↑	0.4653 ± 0.0467	0.4754 ± 0.0357	0.4777 ± 0.0049	0.4459 ± 0.0011	**0.5215 ± 0.0200**	0.4884 ± 0.0000	0.4593 ± 0.0016

Texture	FCM	MEC	FSC	2PFCM	BFC	KFCM	CAFCM
WGSS↓	16.0626 ± 0.1793	51.2179 ± 2.9583	33.7848 ± 3.5161	16.0031 ± 0.0000	×	43.7941 ± 1.8668	**15.5734 ± 0.0000**
MRI↓	0.3346 ± 0.0016	0.5275 ± 0.0003	0.8380 ± 0.0074	0.3341 ± 0.0000	×	0.5434 ± 0.0032	**0.3330 ± 0.0000**
GPI↓	0.0084 ± 0.0002	0.0781 ± 0.0002	0.0940 ± 0.0048	0.0083 ± 0.0000	×	0.0892 ± 0.0019	**0.0079 ± 0.0000**
BHGI↑	0.9011 ± 0.0025	0.6874 ± 0.0009	0.1706 ± 0.0110	0.9019 ± 0.0000	×	0.6376 ± 0.0096	**0.9199 ± 0.0000**
CI↓	0.0369 ± 0.0008	0.1366 ± 0.0002	0.3168 ± 0.0044	0.0367 ± 0.0000	×	0.1483 ± 0.0026	**0.0300 ± 0.0000**
TI↑	0.3712 ± 0.0004	**0.4860 ± 0.0006**	0.0812 ± 0.0058	0.3714 ± 0.0000	×	0.4474 ± 0.0097	0.4093 ± 0.0000
DGI↑	0.1211 ± 0.0157	0.0950 ± 0.0019	0.0595 ± 0.0087	0.1263 ± 0.0000	×	0.0953 ± 0.0077	0.0890 ± 0.0000
RLI↑	0.2775 ± 0.0007	**0.3644 ± 0.0394**	0.1894 ± 0.0040	0.2778 ± 0.0000	×	0.2238 ± 0.0036	0.2793 ± 0.0000
CHI↑	7.1204 ± 0.1057	4.4463 ± 1.2798	0.4649 ± 0.0430	7.1556 ± 0.0000	×	1.4389 ± 0.0820	**7.4499 ± 0.0000**
RTI↓	1.0617 ± 0.0051	4.5746 ± 6.3519	42.4433 ± 16.7327	1.0594 ± 0.0000	×	60.9281 ± 28.9960	**0.6144 ± 0.0000**
WGI↑	0.3839 ± 0.0044	0.1331 ± 0.0639	0.0197 ± 0.0169	0.3853 ± 0.0000	×	0.0562 ± 0.0186	0.4123 ± 0.0000
DI↑	0.0165 ± 0.0018	0.0108 ± 0.0000	0.0104 ± 0.0016	0.0170 ± 0.0000	×	0.0109 ± 0.0009	0.0156 ± 0.0000
BHI↑	0.1299 ± 0.0011	0.2549 ± 0.0609	**0.5555 ± 0.0426**	0.1295 ± 0.0000	×	0.1620 ± 0.0066	0.1391 ± 0.0000
PBMI↑	0.4994 ± 0.0208	0.3232 ± 0.1332	0.1040 ± 0.0082	0.4924 ± 0.0000	×	0.0476 ± 0.0038	0.6284 ± 0.0000
XBI↓	0.0101 ± 0.0045	0.0457 ± 0.0000	0.1044 ± 0.0469	0.0086 ± 0.0000	×	0.0433 ± 0.0065	0.0151 ± 0.0000
DBI↓	1.3566 ± 0.0035	1.2662 ± 0.4884	6.2638 ± 0.9078	1.3552 ± 0.0000	×	4.6500 ± 0.7287	1.1756 ± 0.0000
LSSRI↑	1.9628 ± 0.0151	0.1953 ± 0.0020	-0.7804 ± 0.0872	1.9679 ± 0.0000	×	0.3540 ± 0.0498	**2.0082 ± 0.0000**
TWI↓	1.4735 ± 0.0199	5.3993 ± 0.0058	8.2005 ± 0.2295	1.4668 ± 0.0000	×	4.9345 ± 0.1425	**1.4158 ± 0.0000**
ACC↑	0.6330 ± 0.0114	0.1824 ± 0.0003	0.1860 ± 0.0206	0.6367 ± 0.0000	×	0.2036 ± 0.0170	0.5709 ± 0.0000
NMI↑	0.6254 ± 0.0046	0.3779 ± 0.0006	0.1238 ± 0.0232	0.6269 ± 0.0000	×	0.3642 ± 0.0142	0.6313 ± 0.0000
ARI↑	0.5018 ± 0.0102	0.1315 ± 0.0002	0.0376 ± 0.0073	0.5050 ± 0.0000	×	0.1465 ± 0.0120	0.4596 ± 0.0000

Optdigits	KM	KM++	PKM	EWPKM	SC	HC	CAPKM++2.0
WGSS↓	238.0204 ± 3.7684	238.6506 ± 4.5788	235.2651 ± 0.7834	344.0539 ± 5.0062	241.4227 ± 0.0360	237.9126 ± 0.0000	**234.8252 ± 0.0000**
MRI↓	0.7191 ± 0.0094	0.7199 ± 0.0093	**0.7111 ± 0.0025**	0.9429 ± 0.0013	0.7281 ± 0.0015	0.7253 ± 0.0000	**0.7111 ± 0.0000**
GPI↓	0.0189 ± 0.0025	0.0190 ± 0.0026	0.0169 ± 0.0006	0.1919 ± 0.0047	0.0231 ± 0.0005	0.0218 ± 0.0000	**0.0168 ± 0.0000**
BHGI↑	0.8118 ± 0.0201	0.8130 ± 0.0249	0.8237 ± 0.0063	0.2000 ± 0.0057	0.7793 ± 0.0034	0.7862 ± 0.0000	**0.8307 ± 0.0000**
CI↓	0.1176 ± 0.0111	0.1162 ± 0.0138	0.1115 ± 0.0045	0.3780 ± 0.0044	0.1251 ± 0.0014	0.1245 ± 0.0000	**0.1059 ± 0.0000**
TI↑	0.3632 ± 0.0138	0.3669 ± 0.0151	0.3606 ± 0.0087	0.1385 ± 0.0032	0.3568 ± 0.0004	0.3552 ± 0.0000	**0.3701 ± 0.0000**
DGI↑	0.4874 ± 0.0387	0.4926 ± 0.0475	0.4799 ± 0.0476	0.3499 ± 0.0462	**0.6619 ± 0.0100**	0.6114 ± 0.0000	0.4134 ± 0.0000
RLI↑	0.1809 ± 0.0017	0.1809 ± 0.0023	0.1820 ± 0.0004	0.1278 ± 0.0011	0.1785 ± 0.0001	0.1791 ± 0.0000	**0.1821 ± 0.0000**
CHI↑	0.8088 ± 0.0279	0.8042 ± 0.0336	0.8296 ± 0.0060	0.0885 ± 0.0022	0.7446 ± 0.0021	0.7653 ± 0.0000	0.8330 ± 0.0000
RTI↓	1.6654 ± 0.6256	1.4157 ± 0.4323	1.5200 ± 0.2926	17.4298 ± 2.3087	**1.0344 ± 0.0013**	1.0956 ± 0.0000	1.1413 ± 0.0004
WGI↑	0.2767 ± 0.0121	0.2766 ± 0.0151	0.2826 ± 0.0055	0.0089 ± 0.0020	0.2740 ± 0.0003	0.2671 ± 0.0000	**0.2904 ± 0.0000**
DI↑	0.1368 ± 0.0121	0.1405 ± 0.0149	0.1331 ± 0.0139	0.1053 ± 0.0137	**0.1733 ± 0.0024**	0.1692 ± 0.0000	0.1139 ± 0.0000
BHI↑	2.5823 ± 0.0427	2.5976 ± 0.0449	2.5910 ± 0.0087	3.5609 ± 0.0368	2.6041 ± 0.0035	2.6413 ± 0.0000	2.5848 ± 0.0001
PBMI↑	0.1568 ± 0.0067	0.1561 ± 0.0073	0.1547 ± 0.0033	0.1059 ± 0.0047	0.1900 ± 0.0005	0.1596 ± 0.0000	0.1545 ± 0.0001
XBI↓	0.0014 ± 0.0002	0.0013 ± 0.0003	0.0014 ± 0.0003	0.0030 ± 0.0007	**0.0007 ± 0.0000**	0.0008 ± 0.0000	0.0019 ± 0.0000
DBI↓	1.9179 ± 0.0796	1.8986 ± 0.0961	1.9102 ± 0.0474	4.9440 ± 0.2232	**1.8383 ± 0.0047**	1.9093 ± 0.0000	1.8543 ± 0.0002
LSSRI↑	-0.2128 ± 0.0356	-0.2187 ± 0.0433	-0.1869 ± 0.0073	-2.4247 ± 0.0255	-0.2950 ± 0.0029	-0.2675 ± 0.0000	**-0.1827 ± 0.0000**
TWI↓	23.8020 ± 0.3768	23.8651 ± 0.4579	23.5267 ± 0.0783	39.5425 ± 0.0817	24.6730 ± 0.0300	24.3835 ± 0.0000	23.4825 ± 0.0000
ACC↑	0.7537 ± 0.0641	0.7357 ± 0.0528	0.7950 ± 0.0256	0.1741 ± 0.0039	**0.8265 ± 0.0003**	0.8089 ± 0.0000	0.7914 ± 0.0001
NMI↑	0.7342 ± 0.0272	0.7240 ± 0.0255	0.7486 ± 0.0111	0.1355 ± 0.0007	**0.8708 ± 0.0006**	0.8250 ± 0.0000	0.7563 ± 0.0002
ARI↑	0.6355 ± 0.0602	0.6160 ± 0.0507	0.6722 ± 0.0250	0.0150 ± 0.0013	**0.7799 ± 0.0003**	0.7170 ± 0.0000	0.6704 ± 0.0002

Optdigits	FCM	MEC	FSC	2PFCM	BFC	KFCM	CAFCM
WGSS↓	301.2430 ± 10.6738	289.1568 ± 9.2649	387.2978 ± 11.7520	306.0312 ± 0.0000	365.3603 ± 7.7366	287.3822 ± 9.4675	**234.8252 ± 0.0000**
MRI↓	0.8541 ± 0.0154	0.8345 ± 0.0171	0.9156 ± 0.0119	0.8408 ± 0.0000	0.9824 ± 0.0049	0.8318 ± 0.0184	**0.7111 ± 0.0000**
GPI↓	0.0935 ± 0.0161	0.0734 ± 0.0161	0.0576 ± 0.0337	0.0846 ± 0.0000	0.0886 ± 0.0019	0.0683 ± 0.0124	**0.0168 ± 0.0000**
BHGI↑	0.4784 ± 0.0480	0.5364 ± 0.0474	0.3218 ± 0.0492	0.5264 ± 0.0000	0.0517 ± 0.0137	0.5403 ± 0.0571	**0.8307 ± 0.0000**
CI↓	0.2699 ± 0.0217	0.2515 ± 0.0188	0.3031 ± 0.0220	0.2439 ± 0.0000	0.5344 ± 0.0076	0.2534 ± 0.0279	**0.1059 ± 0.0000**
TI↑	0.2844 ± 0.0238	0.2984 ± 0.0179	0.1252 ± 0.0392	0.3146 ± 0.0000	0.0224 ± 0.0060	0.2929 ± 0.0274	**0.3701 ± 0.0000**
DGI↑	0.3498 ± 0.0508	0.3593 ± 0.0487	0.4267 ± 0.0481	0.3305 ± 0.0000	0.2348 ± 0.0281	0.3552 ± 0.0543	0.4135 ± 0.0000
RLI↑	0.1429 ± 0.0101	0.1443 ± 0.0085	0.1151 ± 0.0095	0.1491 ± 0.0000	0.0451 ± 0.0063	0.1427 ± 0.0077	**0.1821 ± 0.0000**
CHI↑	0.4032 ± 0.0668	0.4028 ± 0.0588	0.0376 ± 0.0156	0.4423 ± 0.0000	0.0280 ± 0.0081	0.4001 ± 0.0538	**0.8330 ± 0.0000**
RTI↓	5.1299 ± 2.4365	3.3267 ± 1.2337	3.1296 ± 1.1438	4.9275 ± 0.0000	87.9181 ± 47.4428	3.5445 ± 1.4785	1.1414 ± 0.0000
WGI↑	0.0760 ± 0.0263	0.0830 ± 0.0237	0.0459 ± 0.0267	0.0898 ± 0.0000	0.0000 ± 0.0000	0.0866 ± 0.0251	**0.2904 ± 0.0000**
DI↑	0.1034 ± 0.0149	0.1065 ± 0.0149	0.1325 ± 0.0150	0.0960 ± 0.0000	0.0732 ± 0.0087	0.1060 ± 0.0155	0.1139 ± 0.0000
BHI↑	3.0998 ± 0.2102	3.0147 ± 0.2178	2.8654 ± 0.5831	3.3187 ± 0.0000	**4.6291 ± 0.0381**	3.0222 ± 0.2087	2.5848 ± 0.0000
PBMI↑	0.1806 ± 0.0537	0.1209 ± 0.0293	**0.2901 ± 0.0719**	0.1531 ± 0.0000	0.0066 ± 0.0021	0.1082 ± 0.0231	0.1544 ± 0.0000
XBI↓	0.0029 ± 0.0010	0.0027 ± 0.0010	0.0019 ± 0.0003	0.0030 ± 0.0000	0.0066 ± 0.0013	0.0028 ± 0.0012	0.0019 ± 0.0000
DBI↓	2.9943 ± 0.3742	2.6679 ± 0.2418	2.3283 ± 0.3616	3.3505 ± 0.0000	13.8393 ± 2.0233	2.7372 ± 0.2927	1.8541 ± 0.0000
LSSRI↑	-1.1949 ± 0.1293	-1.0071 ± 0.1217	-3.8470 ± 0.5176	-1.2218 ± 0.0000	-3.6155 ± 0.2831	-0.9709 ± 0.1269	**-0.1827 ± 0.0000**
TWI↓	33.0074 ± 0.9936	31.4988 ± 1.0204	42.0430 ± 0.4150	33.2459 ± 0.0000	41.8754 ± 0.3268	31.1890 ± 1.0839	**23.4825 ± 0.0000**
ACC↑	0.3761 ± 0.0401	0.4079 ± 0.0429	0.1261 ± 0.0110	0.4075 ± 0.0000	0.1788 ± 0.0155	0.4180 ± 0.0434	0.7913 ± 0.0000
NMI↑	0.3846 ± 0.0237	0.4019 ± 0.0276	0.0786 ± 0.0195	0.3960 ± 0.0000	0.0420 ± 0.0130	0.4031 ± 0.0321	0.7560 ± 0.0000
ARI↑	0.2268 ± 0.0278	0.2497 ± 0.0360	0.0024 ± 0.0023	0.2541 ± 0.0000	0.0230 ± 0.0080	0.2554 ± 0.0326	0.6702 ± 0.0000

The best ones are boldfaced and second best ones are underlined.

TABLE V
MEAN VALUES AND STANDARD DEVIATIONS OF INTERNAL AND EXTERNAL CLUSTER VALIDITY INDICES RESULTING FROM CAFCM, AND THIRTEEN BASELINES ON EGS AND LR, WHERE $N = 2$ AND $M = 5$ IN CAPKM++2.0 AND CAFCM ON EGS, AND $N = 3$ AND $M = 15$ IN CAPKM++2.0 AND CAFCM ON LR

EGS	KM	KM++	PKM	EWPKM	SC	HC	CAPKM++2.0
WGSS↓	699.6124 ± 0.3592	699.5962 ± 0.3487	699.4982 ± 0.4711	699.6561 ± 0.0000	700.3543 ± 0.0001	708.1015 ± 0.0000	**699.3998 ± 0.0000**
MRI↓	0.9233 ± 0.0002	0.9233 ± 0.0002	0.9233 ± 0.0006	0.9236 ± 0.0000	0.9270 ± 0.0000	0.9643 ± 0.0000	**0.9231 ± 0.0000**
GPI↓	0.1883 ± 0.0001	0.1883 ± 0.0001	0.1883 ± 0.0005	0.1887 ± 0.0000	0.1914 ± 0.0000	0.2215 ± 0.0000	**0.1882 ± 0.0000**
BHGI↑	0.2466 ± 0.0005	0.2467 ± 0.0004	0.2467 ± 0.0018	0.2452 ± 0.0000	0.2345 ± 0.0000	0.1109 ± 0.0000	**0.2471 ± 0.0000**
CI↓	0.3640 ± 0.0004	0.3639 ± 0.0004	0.3639 ± 0.0010	0.3645 ± 0.0000	0.3708 ± 0.0000	0.4375 ± 0.0000	**0.3637 ± 0.0000**
TI↑	0.1744 ± 0.0003	0.1744 ± 0.0003	0.1745 ± 0.0013	0.1734 ± 0.0000	0.1658 ± 0.0000	0.0783 ± 0.0000	**0.1747 ± 0.0000**
DGI↑	0.3843 ± 0.0609	0.3933 ± 0.0570	0.3486 ± 0.0166	0.4417 ± 0.0000	0.2612 ± 0.0000	**0.5407 ± 0.0000**	0.3449 ± 0.0000
RLI↑	0.2231 ± 0.0034	0.2233 ± 0.0033	0.2242 ± 0.0017	**0.2257 ± 0.0000**	0.2131 ± 0.0000	0.1528 ± 0.0000	0.2246 ± 0.0000
CHI↑	0.0834 ± 0.0006	0.0835 ± 0.0005	0.0836 ± 0.0007	0.0833 ± 0.0000	0.0783 ± 0.0000	0.0401 ± 0.0000	**0.0838 ± 0.0000**
RTI↓	2.9960 ± 0.0201	2.9950 ± 0.0195	2.9899 ± 0.0276	3.0018 ± 0.0000	3.1912 ± 0.0000	5.8545 ± 0.0000	**2.9841 ± 0.0000**
WGI↑	0.1328 ± 0.0003	0.1328 ± 0.0002	0.1328 ± 0.0008	0.1322 ± 0.0000	0.1265 ± 0.0000	0.0720 ± 0.0000	**0.1330 ± 0.0000**
DI↑	0.1005 ± 0.0139	0.1029 ± 0.0121	0.0930 ± 0.0043	0.1184 ± 0.0000	0.0677 ± 0.0000	**0.1427 ± 0.0000**	0.0921 ± 0.0000
BHI↑	0.9095 ± 0.0005	0.9095 ± 0.0005	0.9093 ± 0.0006	0.9096 ± 0.0000	0.9139 ± 0.0000	**0.9408 ± 0.0000**	0.9092 ± 0.0000
PBMI↑	0.0824 ± 0.0005	0.0824 ± 0.0005	0.0825 ± 0.0007	0.0822 ± 0.0000	0.0774 ± 0.0000	0.0422 ± 0.0000	**0.0827 ± 0.0000**
XBI↓	0.0015 ± 0.0005	0.0014 ± 0.0004	0.0017 ± 0.0001	0.0011 ± 0.0000	0.0030 ± 0.0000	**0.0007 ± 0.0000**	0.0017 ± 0.0000
DBI↓	3.4269 ± 0.0109	3.4264 ± 0.0106	3.4236 ± 0.0154	3.4309 ± 0.0000	3.5355 ± 0.0000	4.7719 ± 0.0000	**3.4204 ± 0.0000**
LSSRI↑	-2.4836 ± 0.0067	-2.4833 ± 0.0065	-2.4815 ± 0.009	-2.4855 ± 0.0000	-2.5467 ± 0.0000	-3.2157 ± 0.0000	**-2.4796 ± 0.0000**
TWI↓	349.8062 ± 0.1796	349.7981 ± 0.1744	349.7503 ± 0.2395	349.8587 ± 0.0000	351.4634 ± 0.0002	364.3754 ± 0.0000	**349.6999 ± 0.0000**
ACC↑	0.6190 ± 0.1107	0.6145 ± 0.1085	0.5998 ± 0.0290	0.5015 ± 0.0000	**0.7968 ± 0.0001**	0.6062 ± 0.0000	0.5898 ± 0.0001
NMI↑	0.0941 ± 0.1468	0.0885 ± 0.1443	0.0357 ± 0.0352	0.0000± 0.0000	**0.3139 ± 0.0001**	0.0729 ± 0.0000	0.0262 ± 0.0000
ARI↑	0.1046 ± 0.1599	0.0985 ± 0.1572	0.0430 ± 0.0398	-0.0001 ± 0.0000	**0.3523 ± 0.0002**	0.0406 ± 0.0000	0.0322 ± 0.0001
EGS	FCM	MEC	FSC	2PFCM	BFC	KFCM	CAFCM
WGSS↓	701.7638 ± 2.3880	707.6171 ± 3.8777	713.7808 ± 19.2256	700.2104 ± 0.0000	×	706.7937 ± 3.7233	**699.3998 ± 0.0000**
MRI↓	0.9263 ± 0.0033	0.9344 ± 0.0048	0.9493 ± 0.0346	0.9244 ± 0.0000	×	0.9334 ± 0.0046	**0.9231 ± 0.0000**
GPI↓	0.1908 ± 0.0028	0.1976 ± 0.0040	0.2091 ± 0.0278	0.1893 ± 0.0000	×	0.1968 ± 0.0039	**0.1882 ± 0.0000**
BHGI↑	0.2367 ± 0.0110	0.2095 ± 0.0162	0.1630 ± 0.1117	0.2427 ± 0.0000	×	0.2129 ± 0.0155	**0.2471 ± 0.0000**
CI↓	0.3695 ± 0.0060	0.3842 ± 0.0088	0.4100 ± 0.0613	0.3659 ± 0.0000	×	0.3824 ± 0.0085	**0.3637 ± 0.0000**
TI↑	0.1674 ± 0.0078	0.1481 ± 0.0114	0.1152 ± 0.0790	0.1716 ± 0.0000	×	0.1505 ± 0.0109	**0.1747 ± 0.0000**
DGI↑	0.3672 ± 0.0345	0.3764 ± 0.0380	0.3746 ± 0.0615	0.3332 ± 0.0000	×	0.3769 ± 0.0370	0.3449 ± 0.0000
RLI↑	0.2136 ± 0.0106	0.1894 ± 0.0158	0.1595 ± 0.0861	0.2234 ± 0.0000	×	0.1923 ± 0.0150	0.2246 ± 0.0000
CHI↑	0.0796 ± 0.0041	0.0697 ± 0.0059	0.0522 ± 0.0351	0.0823 ± 0.0000	×	0.0709 ± 0.0057	**0.0838 ± 0.0000**
RTI↓	3.1493 ± 0.1793	3.6117 ± 0.3095	66.5073 ± 141.6230	3.0367 ± 0.0000	×	3.5469 ± 0.2906	**2.9841 ± 0.0000**
WGI↑	0.1282 ± 0.0051	0.1155 ± 0.0076	0.0853 ± 0.0564	0.1310 ± 0.0000	×	0.1171 ± 0.0072	**0.1330 ± 0.0000**
DI↑	0.0960 ± 0.0096	0.0980 ± 0.0104	0.0981 ± 0.0178	0.0865 ± 0.0000	×	0.0979 ± 0.0101	0.0921 ± 0.0000
BHI↑	0.9127 ± 0.0035	0.9212 ± 0.0051	0.9383 ± 0.0293	0.9104 ± 0.0000	×	0.9202 ± 0.0049	0.9092 ± 0.0000
PBMI↑	0.0786 ± 0.0040	0.0688 ± 0.0058	0.0523 ± 0.0350	0.0812 ± 0.0000	×	0.0700 ± 0.0056	**0.0827 ± 0.0000**
XBI↓	0.0016 ± 0.0004	0.0015 ± 0.0003	0.0016 ± 0.0007	0.0019 ± 0.0000	×	0.0015 ± 0.0003	0.0017 ± 0.0000
DBI↓	3.5118 ± 0.0971	3.7587 ± 0.1605	10.6748 ± 12.2112	3.4507 ± 0.0000	×	3.7253 ± 0.1515	**3.4204 ± 0.0000**
LSSRI↑	-2.5320 ± 0.0539	-2.6669 ± 0.0852	-3.8010 ± 1.8519	-2.4971 ± 0.0000	×	-2.6492 ± 0.0809	**-2.4796 ± 0.0000**
TWI↓	351.0553 ± 1.3317	354.3084 ± 1.9544	360.6021 ± 12.3114	350.1689 ± 0.0000	×	353.9031 ± 1.8724	**349.6999 ± 0.0000**
ACC↑	0.6705 ± 0.0998	0.6219 ± 0.0712	0.6703 ± 0.2042	0.5639 ± 0.0000	×	0.6214 ± 0.0813	0.5898 ± 0.0000
NMI↑	0.1361 ± 0.1249	0.0664 ± 0.0659	0.2577 ± 0.361	0.0133 ± 0.0000	×	0.0715 ± 0.0817	0.0262 ± 0.0000
ARI↑	0.1553 ± 0.1377	0.0792 ± 0.0764	0.2784 ± 0.3861	0.0162 ± 0.0000	×	0.0848 ± 0.0940	0.0322 ± 0.0000

LR	KM	KM++	PKM	EWPKM	SC	HC	CAPKM++2.0
WGSS↓	172.2610 ± 1.2342	172.2106 ± 1.2526	172.5354 ± 0.8054	285.7491 ± 1.2048	320.8225 ± 3.7651	177.5555 ± 0.0000	169.7897 ± 0.094
MRI↓	0.5847 ± 0.0037	0.5843 ± 0.0033	0.5844 ± 0.0018	0.8217 ± 0.0012	0.8209 ± 0.0086	0.6268 ± 0.0000	**0.5804 ± 0.0014**
GPI↓	0.0070 ± 0.0003	0.0070 ± 0.0003	0.0068 ± 0.0001	0.0358 ± 0.0006	0.1081 ± 0.0113	0.0131 ± 0.0000	**0.0067 ± 0.0002**
BHGI↑	0.8367 ± 0.0066	0.8382 ± 0.0055	0.8341 ± 0.0040	0.3671 ± 0.0028	0.4255 ± 0.0235	0.7685 ± 0.0000	**0.8458 ± 0.0022**
CI↓	0.1072 ± 0.0034	0.1063 ± 0.0029	0.1092 ± 0.0021	0.3042 ± 0.0011	0.2975 ± 0.0098	0.1304 ± 0.0000	0.1025 ± 0.0009
TI↑	0.2446 ± 0.0044	0.2466 ± 0.0049	0.2382 ± 0.0033	0.1235 ± 0.0014	0.2602 ± 0.0107	0.2590 ± 0.0000	0.2497 ± 0.0019
DGI↑	0.2086 ± 0.0051	0.2084 ± 0.0045	0.2093 ± 0.0046	0.1637 ± 0.0007	**0.3352 ± 0.0058**	0.2015 ± 0.0000	0.2088 ± 0.0011
RLI↑	0.1528 ± 0.0003	0.1529 ± 0.0004	0.1529 ± 0.0002	0.1061 ± 0.0002	0.0817 ± 0.0026	0.1481 ± 0.0000	**0.1534 ± 0.0000**
CHI↑	1.7576 ± 0.0197	1.7584 ± 0.0201	1.7531 ± 0.0129	0.4214 ± 0.0020	0.2304 ± 0.0177	1.4861 ± 0.0000	1.7976 ± 0.0015
RTI↓	1.2844 ± 0.1338	1.2616 ± 0.1410	1.4320 ± 0.1503	18.7362 ± 2.7223	4.2300 ± 0.3628	1.9338 ± 0.0000	1.1236 ± 0.0278
WGI↑	0.2420 ± 0.0046	0.2434 ± 0.0054	0.2391 ± 0.0029	0.0021 ± 0.0004	0.0891 ± 0.0077	0.1982 ± 0.0000	0.2494 ± 0.0024
DI↑	0.0455 ± 0.0010	0.0456 ± 0.0010	0.0456 ± 0.0007	0.0408 ± 0.0000	**0.0623 ± 0.0011**	0.0405 ± 0.0000	0.0446 ± 0.0011
BHI↑	0.1399 ± 0.0023	0.1395 ± 0.0022	0.1409 ± 0.0012	0.2665 ± 0.0020	0.0572 ± 0.0040	0.1380 ± 0.0000	0.1382 ± 0.0014
PBMI↑	**0.0061 ± 0.0004**	**0.0061 ± 0.0004**	**0.0061 ± 0.0002**	0.0042 ± 0.0002	0.0040 ± 0.0001	0.0059 ± 0.0000	0.0059 ± 0.0000
XBI↓	0.0016 ± 0.0000	0.0015 ± 0.0000	0.0016 ± 0.0000	0.0030 ± 0.0000	**0.0009 ± 0.0000**	0.0017 ± 0.0000	0.0015 ± 0.0000
DBI↓	1.6843 ± 0.0403	1.6787 ± 0.0419	1.7244 ± 0.0275	6.1901 ± 0.1554	**1.0860 ± 0.0279**	1.7262 ± 0.0000	1.6366 ± 0.0269
LSSRI↑	0.5639 ± 0.0112	0.5643 ± 0.0114	0.5614 ± 0.0073	-0.8641 ± 0.0048	-1.4710 ± 0.0775	0.3961 ± 0.0000	0.5864 ± 0.0009
TWI↓	6.6254 ± 0.0475	6.6235 ± 0.0482	6.6361 ± 0.0310	12.8526 ± 0.0184	14.8516 ± 0.2144	7.3487 ± 0.0000	6.5304 ± 0.0036
ACC↑	0.2561 ± 0.0097	0.2582 ± 0.0087	**0.2621 ± 0.0061**	0.0943 ± 0.0011	0.1279 ± 0.0114	0.2600 ± 0.0000	0.2574 ± 0.0048
NMI↑	0.3562 ± 0.0051	0.3538 ± 0.0058	0.3528 ± 0.0037	0.0685 ± 0.0012	0.2703 ± 0.0235	**0.4082 ± 0.0000**	0.3608 ± 0.0011
ARI↑	0.1319 ± 0.0057	0.1317 ± 0.0055	**0.1367 ± 0.0035**	0.0152 ± 0.0003	0.0075 ± 0.0026	0.1293 ± 0.0000	0.1294 ± 0.0024
LR	FCM	MEC	FSC	2PFCM	BFC	KFCM	CAFCM
WGSS↓	303.7112 ± 20.1367	257.0694 ± 8.1591	313.2757 ± 13.1218	314.2095 ± 0.0000	300.3002 ± 15.1015	240.5271 ± 7.1036	**169.6638 ± 0.0000**
MRI↓	0.8241 ± 0.0063	0.8017 ± 0.0136	0.9774 ± 0.0202	0.8390 ± 0.0000	0.9356 ± 0.0113	0.7822 ± 0.0172	0.5805 ± 0.0000
GPI↓	0.1415 ± 0.0062	0.1117 ± 0.0165	0.1657 ± 0.0108	0.1339 ± 0.0000	0.0353 ± 0.0012	0.0782 ± 0.0181	0.0068 ± 0.0000
BHGI↑	0.3968 ± 0.0179	0.4440 ± 0.0293	0.0432 ± 0.0425	0.3554 ± 0.0000	0.1331 ± 0.0229	0.4781 ± 0.0358	0.8456 ± 0.0000
CI↓	0.2807 ± 0.0084	0.2571 ± 0.0129	0.4552 ± 0.0218	0.3007 ± 0.0000	0.4027 ± 0.0092	0.2450 ± 0.0146	**0.1022 ± 0.0000**
TI↑	0.2722 ± 0.0193	**0.2796 ± 0.0117**	0.0253 ± 0.0247	0.2291 ± 0.0000	0.0380 ± 0.0066	0.2582 ± 0.0158	0.2508 ± 0.0000
DGI↑	0.1660 ± 0.0128	0.1806 ± 0.0065	0.1476 ± 0.0085	0.1204 ± 0.0000	0.0000± 0.0000	0.1861 ± 0.0041	0.2073 ± 0.0000
RLI↑	0.1034 ± 0.0133	0.1234 ± 0.0079	0.0635 ± 0.0044	0.1118 ± 0.0000	0.0589 ± 0.0064	0.1252 ± 0.0060	**0.1534 ± 0.0000**
CHI↑	0.4078 ± 0.1115	0.6385 ± 0.0991	0.1026 ± 0.0152	0.4931 ± 0.0000	0.1064 ± 0.0256	0.7139 ± 0.0875	**1.7997 ± 0.0000**
RTI↓	91.3596 ± 73.4346	9.9121 ± 5.4788	27.6427 ± 11.5610	197.5310 ± 0.0000	129.7907 ± 73.5306	5.2486 ± 1.7978	**1.0954 ± 0.0000**
WGI↑	0.0172 ± 0.0208	0.0068 ± 0.0060	0.0008 ± 0.0006	0.0239 ± 0.0000	0.0000± 0.0000	0.0195 ± 0.0092	**0.2523 ± 0.0000**
DI↑	0.0353 ± 0.0004	0.0368 ± 0.0010	0.0299 ± 0.0000	0.0351 ± 0.0000	0.0000± 0.0000	0.0376 ± 0.0012	0.0454 ± 0.0000
BHI↑	0.2199 ± 0.0577	0.1615 ± 0.0115	0.2843 ± 0.0217	0.1752 ± 0.0000	**0.3495 ± 0.0092**	0.1584 ± 0.0105	0.1381 ± 0.0000
PBMI↑	0.0028 ± 0.0018	0.0035 ± 0.0008	0.0034 ± 0.0011	0.0041 ± 0.0000	0.0005 ± 0.0002	0.0030 ± 0.0010	0.0060 ± 0.0000
XBI↓	0.0033 ± 0.0001	0.0029 ± 0.0001	0.0039 ± 0.0000	0.0032 ± 0.0000	Inf ± NaN	0.0026 ± 0.0001	0.0015 ± 0.0000
DBI↓	8.3490 ± 4.9826	2.7479 ± 0.2600	5.8008 ± 0.4879	8.2692 ± 0.0000	11.0919 ± 2.4470	2.4005 ± 0.1712	1.6390 ± 0.0000
LSSRI↑	-1.2400 ± 0.1030	-0.7709 ± 0.1309	-2.4892 ± 0.1160	-1.0931 ± 0.0000	-2.2693 ± 0.2487	-0.4841 ± 0.1146	**0.5876 ± 0.0000**
TWI↓	14.1600 ± 0.3321	12.4791 ± 0.5243	16.8622 ± 0.1510	13.6830 ± 0.0000	16.5212 ± 0.3803	11.2964 ± 0.4874	**6.5255 ± 0.0000**
ACC↑	0.0604 ± 0.0046	0.0962 ± 0.0122	0.1146 ± 0.0086	0.0584 ± 0.0000	0.1052 ± 0.0105	0.1259 ± 0.0135	0.2501 ± 0.0000
NMI↑	0.0269 ± 0.0162	0.1155 ± 0.0293	0.1304 ± 0.0209	0.0162 ± 0.0000	0.0513 ± 0.0108	0.1656 ± 0.0270	0.3622 ± 0.0000
ARI↑	0.0032 ± 0.0022	0.0149 ± 0.0091	0.0301 ± 0.0091	0.0033 ± 0.0000	0.0179 ± 0.0046	0.0299 ± 0.0130	0.1287 ± 0.0000

The best ones are boldfaced and second best ones are underlined.

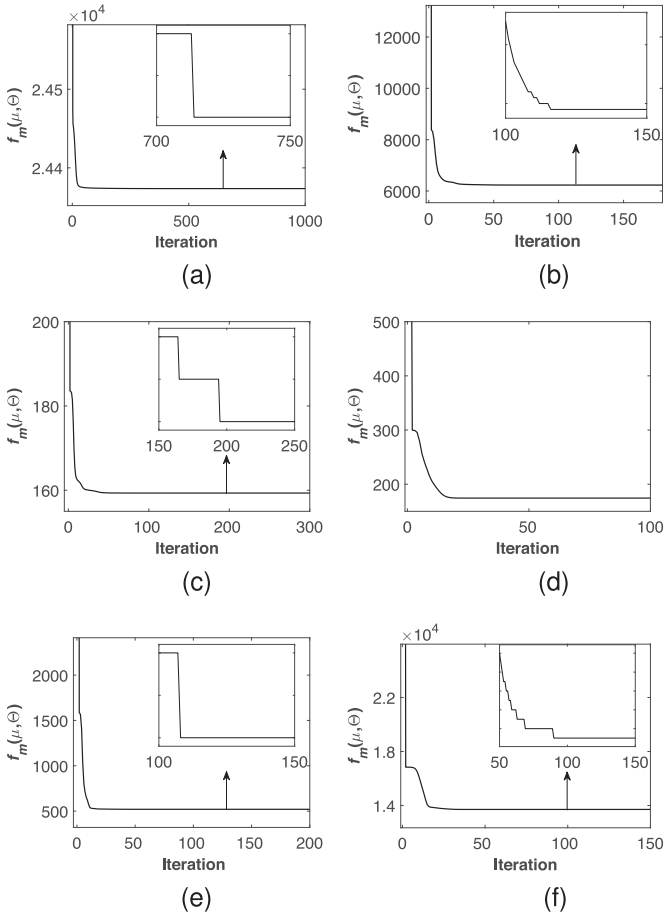

Fig. 6. Snapshots of the fuzzy objective function values of $f_m(\mu, \Theta)$ in (2) with $m = 1.5$ in the FCM clustering loop of CAFCM (Steps 6–10) on the six datasets. (a) NCI9. (b) WarpPIE10P. (c) WineQuality-White. (d) PageBlock. (e) Texture. (f) Optdigits.

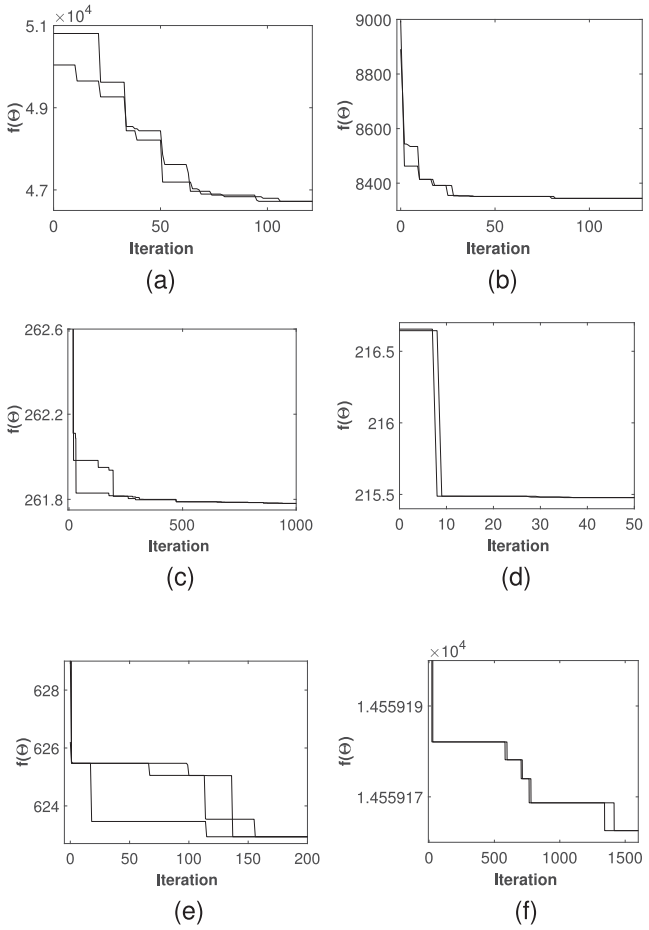

Fig. 7. Descending objective function values of $f(\Theta)$ in the annealing loop of CAFCM (Steps 2–33) on the six datasets. (a) NCI9 ($N = 2$ and $M = 10$). (b) WarpPIE10P ($N = 2$ and $M = 5$). (c) WineQuality-White ($N = 2$ and $M = 15$). (d) PageBlocks ($N = 2$ and $M = 5$). (e) Texture ($N = 3$ and $M = 15$). (f) Optidigits ($N = 2$ and $M = 5$).

3 second-best means (i.e., 13.69% and 15.48%). Fig. 8 depicts the counts of the best and best plus second-best index mean values by using CAFCM and the thirteen baselines. As shown in Fig. 8, CAFCM, CAPKM+++2.0, and SC rank in the first three places in terms of the counts of the best index mean values. CAFCM, CAPKM+++2.0, and PKM rank in the first three places in terms of the counts of best plus second-best index mean values. In addition, the standard deviations of the results using CAFCM are zero, indicating the highest consistency of the algorithm.

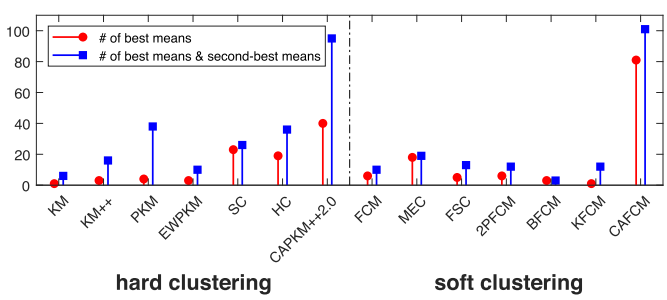

Fig. 8. Counts of the best and best plus second-best index mean values using CAFCM and the thirteen baselines.

E. Complexity Analysis

As shown in Tables I and Table S-II in the Supplementary Materials, the suitable number of modules N is 2 or 3, for 18 datasets with various values of n, p, and k. As N is a small constant, the spatial complexity of CAFCM is the same as FCM (i.e., $O((n+p)k)$ [66]).

The time complexity is empirically estimated via non-negative least-squares regression using the numbers of iterations on the 18 datasets

$$\min_{w} ||Cw - T||_2^2$$
$$\text{s.t. } w \geq 0,$$

where $w \in \Re^{38}$ is the weight vector of the terms, $T \in \Re^{18}$ is the vector of iteration counts, and $C \in \Re^{18\times 38}$ is the matrix of 38 combinations of polynomials and logarithms of n, m, and p. Table S-VIII in the Supplementary Materials lists the 38 combinations of polynomials and logarithms of n, m, and p, and their estimated coefficients. By neglecting the terms with their coefficients w smaller than 0.0001, the resulting estimate is $2\,288\,239\,k^2np + 351\,783\,k^2np\log(p)$. As the second term is of higher order, the estimated time complexity of CAFCM is

$O(k^2np\log(p))$. As the time complexity of FCM is $O(k^2np)$ per iteration [66], it is $\log(p)$ times that of FCM.

V. Conclusion

In this paper, a collaborative annealing fuzzy c-means clustering algorithm is proposed. The experimental results on eight datasets demonstrate that the proposed algorithm with only two or three modules statistically outperforms thirteen competing algorithms in terms of many cluster validity indices. The proposed method achieves superior performance, owing to the adoption of the annealing procedure to phase out fuzziness, as well as collaborative modules to maximize clustering quality and eliminate the influence of initial solutions on clustering performance. Further research may include improving the efficiency of the proposed method, extending it for robust clustering to cluster data in the presence of noises or outliers, extending it for semisupervised clustering to leverage information from labeled and unlabeled data, extending it for multiview clustering to take into account multiple perspectives or representations of data, and applying it to specific problems in science and engineering.

References

[1] A. K. Jain, M. N. Murty, and P. J. Flynn, "Data clustering: A review," *ACM Comput. Surv.*, vol. 31, no. 3, pp. 264–323, 1999.

[2] A. K. Jain, "Data clustering: 50 years beyond k-means," *Pattern Recognit. Lett.*, vol. 31, no. 8, pp. 651–666, 2010.

[3] R. Xu and D. Wunsch, "Survey of clustering algorithms," *IEEE Trans. Neural Netw.*, vol. 16, no. 3, pp. 645–678, May 2005.

[4] X. Peng, J. Feng, J. T. Zhou, Y. Lei, and S. Yan, "Deep subspace clustering," *IEEE Trans. Neural Netw. Learn. Syst.*, vol. 31, no. 12, pp. 5509–5521, Dec. 2020.

[5] S. Zeng, X. Duan, H. Li, J. Bai, Y. Tang, and Z. Wang, "A sparse framework for robust possibilistic k-subspace clustering," *IEEE Trans. Fuzzy Syst.*, vol. 31, no. 4, pp. 1124–1138, Apr. 2023.

[6] L. Jing, M. K. Ng, and J. Z. Huang, "An entropy weighting k-means algorithm for subspace clustering of high-dimensional sparse data," *IEEE Trans. Knowl. Data Eng.*, vol. 19, no. 8, pp. 1026–1041, Aug. 2007.

[7] S. Chakraborty, D. Paul, S. Das, and J. Xu, "Entropy weighted power k-means clustering," in *Proc. Int. Conf. Artif. Intell. Statist.*, 2020, pp. 691–701.

[8] S. Chakraborty and S. Das, "Detecting meaningful clusters from high-dimensional data: A strongly consistent sparse center-based clustering approach," *IEEE Trans. Pattern Anal. Mach. Intell.*, vol. 44, no. 6, pp. 2894–2908, Jun. 2023.

[9] J. B. M. Benjamin and M.-S. Yang, "Weighted multiview possibilistic c-means clustering with L2 regularization," *IEEE Trans. Fuzzy Syst.*, vol. 30, no. 5, pp. 1357–1370, May 2022.

[10] J. Yang and C.-T. Lin, "Multi-view adjacency-constrained hierarchical clustering," *IEEE Trans. Emerg. Topics Comput. Intell.*, vol. 7, no. 4, pp. 1126–1138, Aug. 2023.

[11] P. M.-Smith, W. Williams, M. Dale, and L. Mockett, "Dissimilarity analysis: A new technique of hierarchical sub-division," *Nature*, vol. 202, no. 4936, pp. 1034–1035, 1964.

[12] S. C. Johnson, "Hierarchical clustering schemes," *Psychometrika*, vol. 32, no. 3, pp. 241–254, 1967.

[13] S. Lloyd, "Least squares quantization in PCM," *IEEE Trans. Inf. Theory*, vol. 28, no. 2, pp. 129–137, Mar. 1982.

[14] J. Wang, "A linear assignment clustering algorithm based on the least similar cluster representatives," *IEEE Trans. Syst., Man Cybern., Part A: Syst. Hum.*, vol. 29, no. 1, pp. 100–104, Jan. 1999.

[15] M. Tiwari, M. J. Zhang, J. Mayclin, S. Thrun, C. Piech, and I. Shomorony, "Banditpam: Almost linear time k-medoids clustering via multi-armed bandits," in *Proc. Adv. Neural Inf. Process. Syst.*, 2020, pp. 10211–10222.

[16] B. Zhang, "Generalized k-harmonic means–dynamic weighting of data in unsupervised learning," in *Proc. SIAM Int. Conf. Data Mining*, 2001, pp. 1–13.

[17] J. Shi and J. Malik, "Normalized cuts and image segmentation," *IEEE Trans. Pattern Anal. Mach. Intell.*, vol. 22, no. 8, pp. 888–905, Aug. 2000.

[18] A. Ng, M. Jordan, and Y. Weiss, "On spectral clustering: Analysis and an algorithm," in *Proc. Adv. Neural Inf. Process. Syst.*, 2001, pp. 849–856.

[19] Q. Wang, Z. Qin, F. Nie, and X. Li, "Spectral embedded adaptive neighbors clustering," *IEEE Trans. Neural Netw. Learn. Syst.*, vol. 30, no. 4, pp. 1265–1271, Apr. 2019.

[20] J. Bilmes, "A gentle tutorial of the EM algorithm and its application to parameter estimation for Gaussian mixture and hidden Markov models," Int. Comput. Sci. Inst., Tech. Rep. TR-97-021, 1997.

[21] D. Comaniciu and P. Meer, "Mean shift: A robust approach toward feature space analysis," *IEEE Trans. Pattern Anal. Mach. Intell.*, vol. 24, no. 5, pp. 603–619, May 2002.

[22] A. Bechini, F. Marcelloni, and A. Renda, "TSF-DBSCAN: A novel fuzzy density-based approach for clustering unbounded data streams," *IEEE Trans. Fuzzy Syst.*, vol. 30, no. 3, pp. 623–637, Mar. 2022.

[23] A. Cornuéjols, C. Wemmert, P. Gançarski, and Y. Bennani, "Collaborative clustering: Why, when, what and how," *Inf. Fusion*, vol. 39, pp. 81–95, 2018.

[24] X. Yang, C. Deng, Z. Dang, and D. Tao, "Deep multiview collaborative clustering," *IEEE Trans. Neural Netw. Learn. Syst.*, vol. 34, no. 1, pp. 516–526, Jan. 2023.

[25] J. Xu and K. Lange, "Power k-means clustering," in *Proc. Int. Conf. Mach. Learn.*, 2019, pp. 6921–6931.

[26] H. Li and J. Wang, "Collaborative annealing power k-means clustering," *Knowl.-Based Syst.*, vol. 255, 2022, Art. no. 109593.

[27] H. Li and J. Wang, "CAPKM 2.0: An upgraded version of the collaborative annealing power k-means clustering algorithm," *Knowl.-Based Syst.*, vol. 262, 2023, Art. no. 110241.

[28] R. Krishnapuram and J. M. Keller, "A possibilistic approach to clustering," *IEEE Trans. Fuzzy Syst.*, vol. 1, no. 2, pp. 98–110, May 1993.

[29] E. H. Ruspini, J. C. Bezdek, and J. M. Keller, "Fuzzy clustering: A historical perspective," *IEEE Comput. Intell. Mag.*, vol. 14, no. 1, pp. 45–55, Feb. 2019.

[30] M.-S. Yang and C.-Y. Lai, "A robust automatic merging possibilistic clustering method," *IEEE Trans. Fuzzy Syst.*, vol. 19, no. 1, pp. 26–41, Feb. 2011.

[31] K. D. Koutroumbas, S. D. Xenaki, and A. A. Rontogiannis, "On the convergence of the sparse possibilistic c-means algorithm," *IEEE Trans. Fuzzy Syst.*, vol. 26, no. 1, pp. 324–337, Feb. 2018.

[32] J. C. Bezdek, *Pattern Recognition With Fuzzy Objective Function Algorithms*. New York, NY, USA: Plenum Press, 1981.

[33] Y. Lin and S. Chen, "A centroid auto-fused hierarchical fuzzy c-means clustering," *IEEE Trans. Fuzzy Syst.*, vol. 29, no. 7, pp. 2006–2017, Jul. 2021.

[34] Z. Bian, F.-L. Chung, and S. Wang, "Fuzzy density peaks clustering," *IEEE Trans. Fuzzy Syst.*, vol. 29, no. 7, pp. 1725–1738, Jul. 2021.

[35] J. Zhou, W. Pedrycz, C. Gao, Z. Lai, J. Wan, and Z. Ming, "Robust jointly sparse fuzzy clustering with neighborhood structure preservation," *IEEE Trans. Fuzzy Syst.*, vol. 30, no. 4, pp. 1073–1087, Apr. 2022.

[36] S. Song, Z. Jia, J. Yang, and N. Kasabov, "Image segmentation based on fuzzy low-rank structural clustering," *IEEE Trans. Fuzzy Syst.*, vol. 31, no. 7, pp. 2153–2166, Jul. 2023.

[37] Q. Chen, F. Nie, W. Yu, and X. Li, "$\ell_{2,p}$-Norm and Mahalanobis distance based robust fuzzy c-means," *IEEE Trans. Fuzzy Syst.*, vol. 31, no. 9, pp. 2904–2916, Sep. 2023.

[38] D. L. Pham and J. L. Prince, "An adaptive fuzzy c-means algorithm for image segmentation in the presence of intensity inhomogeneities," *Pattern Recognit. Lett.*, vol. 20, no. 1, pp. 57–68, 1999.

[39] R. J. Hathaway, J. C. Bezdek, and Y. Hu, "Generalized fuzzy c-means clustering strategies using l_p norm distances," *IEEE Trans. Fuzzy Syst.*, vol. 8, no. 5, pp. 576–582, Oct. 2000.

[40] L. Szilagyi, Z. Benyo, S. M. Szilágyi, and H. Adam, "MR brain image segmentation using an enhanced fuzzy c-means algorithm," in *Proc. IEEE 25th Annu. Int. Conf. Eng. Med. Biol. Soc.*, 2003, pp. 724–726.

[41] W. Cai, S. Chen, and D. Zhang, "Fast and robust fuzzy c-means clustering algorithms incorporating local information for image segmentation," *Pattern Recognit.*, vol. 40, no. 3, pp. 825–838, 2007.

[42] C.-H. Li, W.-C. Huang, B.-C. Kuo, and C.-C. Hung, "A novel fuzzy weighted c-means method for image classification," *Int. J. Fuzzy Syst.*, vol. 10, no. 3, pp. 168–173, 2008.

[43] C.-C. Hung, S. Kulkarni, and B.-C. Kuo, "A new weighted fuzzy c-means clustering algorithm for remotely sensed image classification," *IEEE J. Sel. Topics Signal Process.*, vol. 5, no. 3, pp. 543–553, Jun. 2011.

[44] L. Zhu, F.-L. Chung, and S. Wang, "Generalized fuzzy c-means clustering algorithm with improved fuzzy partitions," *IEEE Trans. Syst., Man, Cybern., Part B. (Cybern.)*, vol. 39, no. 3, pp. 578–591, Jun. 2009.
[45] S. Krinidis and V. Chatzis, "A robust fuzzy local information c-means clustering algorithm," *IEEE Trans. Image Process.*, vol. 19, no. 5, pp. 1328–1337, May 2010.
[46] T. C. Glenn, A. Zare, and P. D. Gader, "Bayesian fuzzy clustering," *IEEE Trans. Fuzzy Syst.*, vol. 23, no. 5, pp. 1545–1561, Oct. 2015.
[47] J. Fan, J. Wang, and M. Han, "Cooperative coevolution for large-scale optimization based on kernel fuzzy clustering and variable trust region methods," *IEEE Trans. Fuzzy Syst.*, vol. 22, no. 4, pp. 829–839, Aug. 2014.
[48] T. W. Cheng, D. B. Goldgof, and L. O. Hall, "Fast fuzzy clustering," *Fuzzy Sets Syst.*, vol. 93, no. 1, pp. 49–56, 1998.
[49] H. Hou and S. Liu, "An improved fuzzy c-means algorithm based on genetic algorithm," *Comput. Eng.*, vol. 31, no. 17, pp. 152–154, 2005.
[50] J. Yu, P. Guo, P. Chen, Z. Zhang, and W. Ruan, "Remote sensing image classification based on improved fuzzy c-means," *Geo-Spatial Inf. Sci.*, vol. 11, no. 2, pp. 90–94, 2008.
[51] D.-W. Kim, K. H. Lee, and D. Lee, "A novel initialization scheme for the fuzzy c-means algorithm for color clustering," *Pattern Recognit. Lett.*, vol. 25, no. 2, pp. 227–237, 2004.
[52] K. S. Tan, W. H. Lim, and N. A. M. Isa, "Novel initialization scheme for fuzzy c-means algorithm on color image segmentation," *Appl. Soft Comput.*, vol. 13, no. 4, pp. 1832–1852, 2013.
[53] H. Yang, J. Peng, B. Xia, and D. Zhang, "Remote sensing classification using fuzzy c-means clustering with spatial constraints based on Markov random field," *Eur. J. Remote Sens.*, vol. 46, no. 1, pp. 305–316, 2013.
[54] J. Fan and J. Wang, "A two-phase fuzzy clustering algorithm based on neurodynamic optimization with its application for PolSAR image segmentation," *IEEE Trans. Fuzzy Syst.*, vol. 26, no. 1, pp. 72–83, Feb. 2018.
[55] M. N. Ahmed, S. M. Yamany, N. Mohamed, A. A. Farag, and T. Moriarty, "A modified fuzzy c-means algorithm for bias field estimation and segmentation of MRI data," *IEEE Trans. Med. Imag.*, vol. 21, no. 3, pp. 193–199, Mar. 2002.
[56] S. Chen and D. Zhang, "Robust image segmentation using FCM with spatial constraints based on new kernel-induced distance measure," *IEEE Trans. Syst., Man, Cybern., Part B. (Cybernetics)*, vol. 34, no. 4, pp. 1907–1916, 2004.
[57] J. C. Dunn, "A fuzzy relative of the ISODATA process and its use in detecting compact well-separated clusters," *J. Cybern.*, vol. 3, no. 3, pp. 32–57, 1973.
[58] J. Kennedy and R. Eberhart, "Particle swarm optimization," in *Proc. Int. Conf. Neural Netw.*, 1995, pp. 1942–1948.
[59] H. Che, J. Wang, and A. Cichocki, "Sparse signal reconstruction via collaborative neurodynamic optimization," *Neural Netw.*, vol. 154, pp. 255–269, 2022.
[60] J. Li et al., "Feature selection: A data perspective," *ACM Comput. Surv.*, vol. 50, no. 6, pp. 1–45, 2018.
[61] J. A.-Fdez et al., "KEEL data-mining software tool: Data set repository, integration of algorithms and experimental analysis framework," *J. Mult.-Valued Log. Soft Comput.*, vol. 17, pp. 255–287, 2011.
[62] V. Arzamasov, K. Böhm, and P. Jochem, "Towards concise models of grid stability," in *Proc. IEEE Int. Conf. Commun., Control, Comput. Technol. Smart Grids*, 2018, pp. 1–6.
[63] P. W. Frey and D. J. Slate, "Letter recognition using Holland-style adaptive classifiers," *Mach. Learn.*, vol. 6, pp. 161–182, 1991.
[64] G. Gan and J. Wu, "A convergence theorem for the fuzzy subspace clustering (FSC) algorithm," *Pattern Recognit.*, vol. 41, no. 6, pp. 1939–1947, 2008.
[65] R.-P. Li and M. Mukaidono, "A maximum-entropy approach to fuzzy clustering," in *Proc. IEEE Int. Conf. Fuzzy Syst.*., 1995, pp. 2227–2232.
[66] T. C. Havens, J. C. Bezdek, C. Leckie, L. O. Hall, and M. Palaniswami, "Fuzzy c-means algorithms for very large data," *IEEE Trans. Fuzzy Syst.*, vol. 20, no. 6, pp. 1130–1146, Dec. 2012.

Hongzong Li received the B.E. degree in automation from Northeastern University, Shenyang, China, in 2020. He is currently working toward the Ph.D. degree in computer science with the City University of Hong Kong, Hong Kong.

His current research interests include optimization, computational intelligence, and clustering.

Jun Wang (Life Fellow, IEEE) received his B.S. and M.S. degrees from Dalian University of Technology, Dalian, China, in 1982 and 1985, respectively, and his Ph.D. degree from Case Western Reserve University, Cleveland, OH, USA, in 1991, all in electrical and systems engineering.

He was in various academic positions with Dalian University of Technology, Case Western Reserve University, University of North Dakota, and the Chinese University of Hong Kong. He was also in various short-term or part-time visiting positions with the U.S. Air Force Armstrong Laboratory, Dayton, OH, USA, RIKEN Brain Science Institute, Tokyo, Japan, Huazhong University of Science and Technology, Wuhan, China; Shanghai Jiao Tong University, Shanghai, China, Dalian University of Technology, and Swinburne University of Technology, Melbourne, Australia. He is currently a Chair Professor with City University of Hong Kong, Hong Kong.

Dr. Wang was the recipient of several awards, such as the Research Excellence Award from the Chinese University of Hong Kong (2008–2009), the Outstanding Achievement Award from Asia-Pacific Neural Network Assembly (2011), the IEEE TRANSACTIONS ON NEURAL NETWORKS Outstanding Paper Award (2011), the Neural Networks Pioneer Award from the IEEE Computational Intelligence Society (2014), and the Norbert Wiener Award from the IEEE Systems, Man and Cybernetics Society (2019). He was the General Chair of the 13th/25th International Conference on Neural Information Processing (2006/2018) and the IEEE World Congress on Computational Intelligence (2008). He is currently an IEEE Systems, Man, and Cybernetics Society Distinguished Lecturer (2017–2022), and was a Distinguished Lecturer of IEEE Computational Intelligence Society (2010–2012, 2014–2016). He was the Editor-in-Chief of IEEE TRANSACTIONS ON CYBERNETICS (2014–2019).